Modulation of the reactivity, stability and substrate- and enantioselectivity of an epoxidation catalyst by noncovalent dynamic attachment of a receptor functionality—aspects on the mechanism of the Jacobsen–Katsuki epoxidation applied to a supramolecular system

Stefán Jónsson,[a] Fabrice G. J. Odille,[a] Per-Ola Norrby[b] and Kenneth Wärnmark*[a]

Received 4th January 2006, Accepted 16th March 2006
First published as an Advance Article on the web 19th April 2006
DOI: 10.1039/b518244a

The synthesis of the components of the dynamic supramolecular hydrogen-bonded catalytic system **2** + **3** is described. The catalytic performance and substrate- and enantioselectivity of Mn(salen) catalyst **2** were investigated in the presence and absence of the Zn(porphyrin) receptor unit **3**. The effects of pyridine and pyridine *N*-oxide donor ligands were also studied. Some aspects on the mechanism of the Jacobsen–Katsuki epoxidation, based on literature observations, are introduced as a means to analyse the behaviour of **2** and its modulation by the formation of macrocycle **1** with **3**. A complete association model of the metal-free system **4** + **5** refutes the earlier assumption that macrocycle **1** is the predominant form of catalyst **2** under the standard epoxidation reaction conditions with **2** + **3**. Evidence are provided that receptor-binding substrates and nonbinding substrates, respectively, are epoxidised by two different catalytic species, or two distinct distributions of species in competitive epoxidations using catalytic system **2** + **3**. The two species are assigned to the *endo* and *exo* faces of the Mn(salen) catalyst in macrocycle **1**, and to equivalently folded oligomeric structures with monomers **2** and **3** in adjacent positions.

Introduction

It is one of the great challenges of modern chemical research to capture the power of natural enzymes to perform catalysis with extraordinary rate enhancements and substrate-, chemo-, regio- and enantioselectivity.[1] Two major lines of research are pursued towards this goal. The more mature one, biomimetic catalysis or enzyme mimetics, seeks to produce models of specific enzyme classes, to acquire detailed understanding of their mechanisms of substrate binding, catalysis and selectivity at all levels.[1e,g] The more recent research field, supramolecular catalysis seeks to produce efficient and selective catalysts with the aid of specific molecular interactions and the principles of supramolecular chemistry.[1c,d,2] While drawing inspiration and knowledge from the natural catalysts the emphasis here is more on the creation and study of superior catalytic systems, and less on their comparison with enzymes in terms of structure and function. However, in terms of catalytic performance, the enzymes still stand as the gold standard to which all designed catalytic systems are measured.

In spite of more than twenty years of research in supramolecular catalysis the success has so far been limited. Although large numbers of interesting systems have been introduced, only very few of those could be called superior catalysts.[3] To date, the main problems involved both in enzyme models and supramolecular catalysts have been catalytic cycle arrest (lack of turnover) and product inhibition. Both of these problems can be overcome in terms of kinetic studies by using a stoichiometric amount or more of the catalyst, but in practical terms they render any system useless as a catalyst.

As a solution to these problems, it has been pointed out that more flexible systems, perhaps assembled by noncovalent forces, might be necessary to attain efficient catalysis.[1c] Further, instead of designing strong receptors endowed with catalytic groups, systems with lower affinity for substrates but which are stabilised in the presence of the transition state of the catalysed reaction should be pursued. This transition state (TS)-induced stabilisation could occur by reinforcement of noncovalent interactions or a rearrangement of the catalytic assembly to a lower energy conformation. Although reasonable, this point has not been much followed up in designed catalytic systems, probably because more flexibility leads to higher uncertainty in the design, and an uncertain design is not the best starting point for the large synthetic investment often required to obtain the catalytic system of study.

We have recently reported on a catalytic dynamic supramolecular system (**2** + **3**, Fig. 1),[4] designed with the aim to address the problems and potential solutions discussed above. The system consists of a catalytic unit, a Mn(salen)Cl complex (**2**), and a Zn(porphyrin) receptor unit (**3**). According to the design principle, the receptor binds to the catalyst by hydrogen-bonding, forming macrocyclic heterodimer **1** where an olefinic substrate bearing a receptor-binding functionality at an appropriate distance from the reactive group can be selectively accommodated and epoxidised. The arrangement of the hydrogen-bonding moieties insures that macrocyclic homodimers cannot be formed. We chose the Jacobsen–Katsuki (J–K) epoxidation[5] as the reaction of study mainly because an epoxidation is a simple structural transformation where the reactant and product differ by only one atom and

[a]*Organic Chemistry, Department of Chemistry, Lund University, P.O. Box 124, SE-221 00, Lund, Sweden. E-mail: Kenneth.Warnmark@organic.lu.se; Fax: (+46) 46 2224119; Tel: (+46) 46 2228127*
[b]*Department of Chemistry, Technical University of Denmark, Kemitorvet, DK-2800, Kgs Lyngby, Denmark*

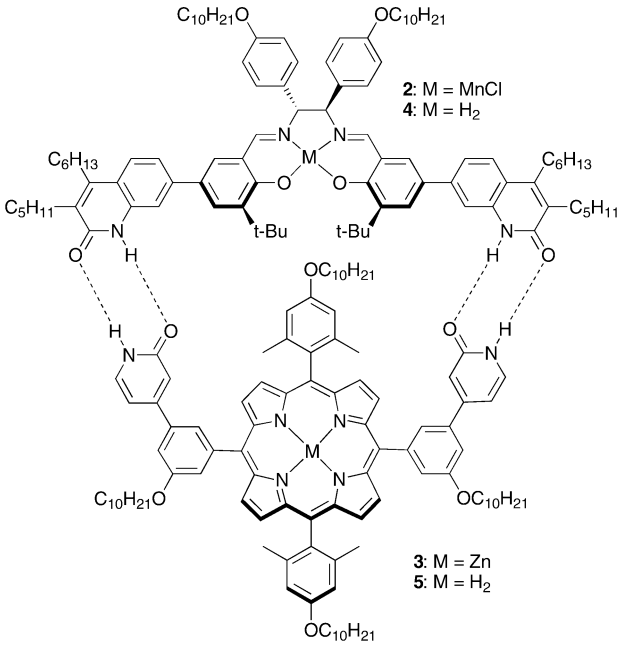

Fig. 1 The macrocyclic heterodimer **1** (**2** + **3**).

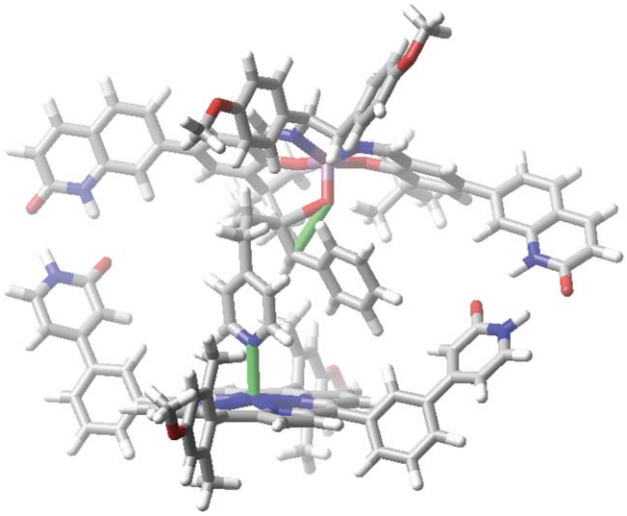

Fig. 2 A molecular mechanics[9] 3D representation of the TS in the epoxidation of a receptor-bound substrate inside the hydrogen-bonded macrocycle **1**. Long alkyl chain substituents are removed for clarity and ease of modelling. Zero-order bonds are coloured green.

the size expansion from substrate to product is unidirectional. The hydrogen-bonding moieties in **2** and **3** are spatially oriented so as to offer directional flexibility in the direction of expansion in the transformation of a bound substrate to product inside macrocycle **1**. Emphasising that assembly and binding events should not be the bottleneck of the catalytic cycle, diffusion controlled[6] association elements were exclusively employed. For substrate binding, the Zn(porphyrin)–pyridine interaction[7] was chosen and for the assembly of the macrocyclic catalyst–receptor complex **1**, the 2-pyridone self-complementary hydrogen-bonding motif[8] was selected. It was thus anticipated that the rather weak hydrogen-bonding interactions would be reinforced by formation of the TS in the epoxidation of a bound substrate. While substrate and product could be expected to bind equally strongly to the receptor unit, the slightly increased size of the epoxide product compared to the substrate was hoped to destabilise the termolecular catalyst–receptor–product complex, and thus drive the turnover cycle forward. Three olefinic substrates (see Scheme 1) were designed and synthesised to test the substrate selectivity of system **2** + **3**, one nonbinding substrate, **6**, and two binding substrates, **7** and **8**, with varying distance between the binding and reacting groups. A three-dimensional molecular mechanics model[9] of macrocycle **1** is shown in Fig. 2, including the TS[10] of the epoxidation of a receptor-bound substrate (**7**) inside the macrocyclic cavity.

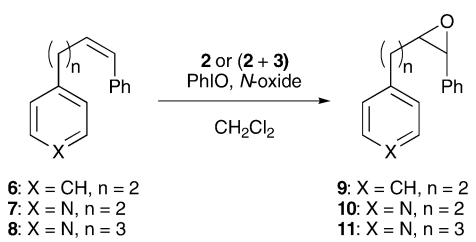

Scheme 1

Since donor ligands such as pyridine *N*-oxides are known to coordinate to the oxygen-donating species in the J–K epoxidation, the design of the catalytic system **1** included a long rigid pyridine *N*-oxide ligand (**12**, see Scheme 8). It was anticipated to coordinate to the *exo* face of the Mn(salen) catalyst, being too large to be accommodated inside the cavity of macrocycle **1**. All catalysis would in this case be forced to occur inside the cavity, on the *endo* face of the catalyst, thus maximising the potential substrate selectivity of the system.

The main conclusions of our previous communication[4] were that supramolecular system **2** + **3** shows low but significant substrate selectivity in pairwise competitive epoxidation experiments. Based on experimental data, the maximum selectivity limit of **1**, when all of **2** is associated to **3**, for substrate **7** *vs* **6** was calculated to be 1.66 and the association constant for the formation of **1** from **2** and **3** was estimated to 2×10^3 M^{-1} with the assumption that **1**, **2** and **3** are the only significant solution species involved. Further, the *N*-oxide ligand **12** was not found to have any important contribution to the observed substrate selectivity.

Although this is neither the first catalytic system that is assembled by hydrogen-bonding[11] nor the first supramolecular encapsulation of a transition metal catalyst,[12] the novelty of the present system lies in the fast assembly and substrate binding processes and its substrate selectivity based on functionality and not only size. We now wish to report the synthesis of its components and further studies into its reactivity, stability and substrate- and enantioselectivity. A complete association model of the metal-free system **4** + **5** representing the real system **2** + **3** is also presented. Since the association behaviour of the system has proven more complicated than previously assumed, we now introduce a modified model in which emphasis is put on catalyst **2** and its hydrogen-bonded aggregates with itself and receptor **3**, including linear oligomers. The proximity between **2** and **3** where they are neighbouring units in a hydrogen-bonded oligomer can explain the apparent significant contribution of such oligomeric residues to the observed substrate selectivity of the catalytic system.

Results and discussion

Synthesis

The molecular structures of both catalyst **2** and receptor **3** are amenable for a convergent modular synthetic approach. The salen ligand **4**, corresponding to catalyst **2**, can be retrosynthetically dismantled into three basic structural modules, a quinolone-based hydrogen-bonding module (**13**), a salicylaldehyde module (**14**) and a diamine module (**15**) *via* a Suzuki cross-coupling and a condensation reaction (Scheme 2). The metal-free porphyrin **5**, corresponding to receptor **3** is similarly broken down into two aromatic aldehydes (**16** and **18**) *via* two consecutive pyrrole condensation reactions, of which **16** is further dissected into a pyridine based hydrogen-bonding module (**19**) and a *meta*-phenylene linker module (**20**) *via* a Stille cross-coupling (Scheme 3). Originally the catalyst and receptor units were prepared without any alkyl substituents. However, these compounds showed an almost complete lack of solubility in any solvent. Alkyl chains were then introduced by way of diamine module **15** and dipyrromethane module **17**, but a practical degree of solubility (*ca.* 2–5 mM) in chlorinated solvents still required the presence of strongly hydrogen-bond competitive cosolvents. Further addition of alkyl substituents resulted in the sufficiently soluble compounds **2** and **3**.

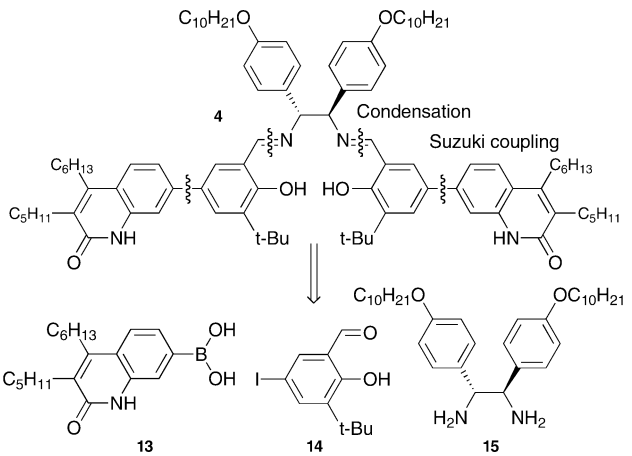

Scheme 2 Retrosynthetic analysis of salen ligand **4**.

For the synthesis of the hydrogen-bonding module **13**, a clever approach to alkylated quinolones was adopted from Zimmerman.[13] Thus, heptanoyl chloride was treated with triethylamine in ether to produce ketene dimer **21**, which was immediately reacted with 3-bromoaniline in refluxing toluene (Scheme 4). The quantitatively formed amide **22** was heated at 80 °C in concentrated sulfuric acid to give a mixture of two compounds from which quinolone **23** could be isolated in 32% yield by recrystallisation. Compound **23** was treated with a large excess of *n*-butyllithium, followed by triisopropyl borate to give, after acidic hydrolysis and a difficult purification, hydrogen-bonding module **13** in 39% yield. Salicylaldehyde module **14** was prepared from 2-*tert*-butylphenol in two steps, *ortho*-formylation followed by iodination, according to published procedures.[14] Modules **13** and **14** could now be assembled in a Suzuki cross-coupling in a refluxing toluene–ethanol–water mixture, providing aldehyde **24** in 60% yield.

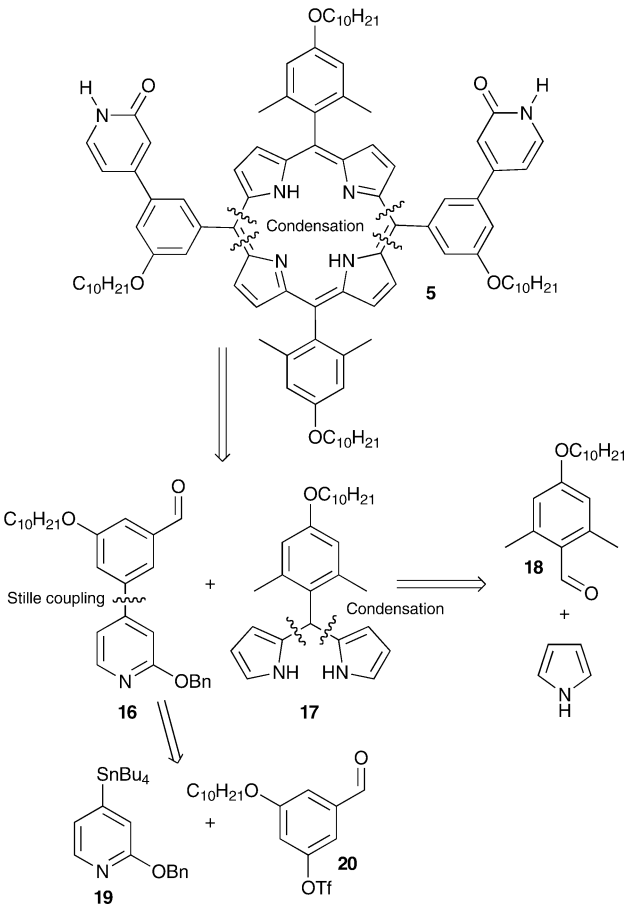

Scheme 3 Retrosynthetic analysis of porphyrin **5**.

Both enantiomers of optically pure diamine **15** were prepared in four steps from 1,2-bis(4-methoxyphenyl)ethane-1,2-diamine **25** (Scheme 4), which was synthesised and resolved following Corey's method.[15] Diamine **25** was first demethylated using BBr_3 in dichloromethane,[16] followed by Boc-protection of the resulting bis(hydroxy)diamine (**26**, Scheme 4). The double *O*-alkylation of protected diamine **27** using potassium carbonate in DMF was unusually sluggish, probably due to the low solubility of the monoalkylated intermediate in the reaction medium. It required THF as a cosolvent and 18-crown-6 as a catalyst to provide **28** in an acceptable 64% yield. The Boc group was quantitatively removed by TFA in dichloromethane, thus completing the synthesis of diamine **15**.

To assemble salen ligand **4**, diamine **15** was condensed with salicylaldehyde **24** in a refluxing 2 : 1 ethanol–toluene mixture in 71% yield (Scheme 4). This is an unusual salen condensation, since the product, which typically precipitates from the reaction mixture, is much more soluble than either of the reactants. Manganese insertion with $Mn(OAc)_2$ and LiCl in a 5 : 2 ethanol–chloroform mixture provided both enantiomers of optically pure catalyst **2** in 94% yield.

2-Fluoro-4-iodopyridine (**34**) was obtained from 2-fluoropyridine *via* two consecutive *ortho*-lithiation steps, iodination in the 3-position followed by a halogen-dance reaction, following a published procedure (Scheme 5).[17] The fluorine atom in **34** was substituted for a benzyloxy group, giving **35** in high yield using benzyl alcohol and KOH with phase transfer catalysis in refluxing

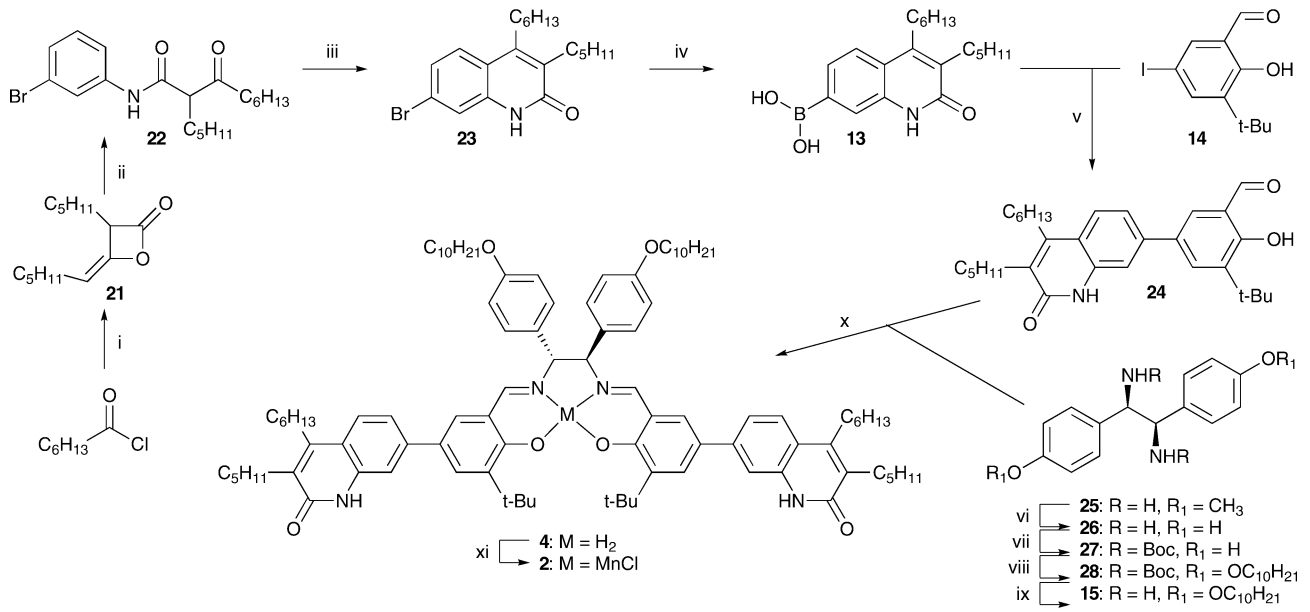

Scheme 4 Synthesis of Mn(salen)Cl complex **2**. (i) Et_3N, Et_2O, rt, 2 h, 85% (crude); (ii) 3-bromoaniline, toluene, reflux, overnight, quant; (iii) conc. H_2SO_4, 80 °C, 2 h, 32%; (iv) 3 equiv. *n*-BuLi, B(O*i*Pr)$_3$, THF, −78 °C to rt, 39%; (v) $Pd(PPh_3)_4$, 2 M aq Na_2CO_3, toluene, EtOH, reflux, 3 h, 60%; (vi) BBr_3, CH_2Cl_2, −78 °C to rt, overnight, 97%; (vii) $(Boc)_2O$, $NaHCO_3$, THF, H_2O, rt, overnight, 64%; (viii) $C_{10}H_{21}Br$, K_2CO_3, 18-crown-6, DMF, THF, 90 °C, 48 h, 64%; (ix) TFA, CH_2Cl_2, rt, 1 h, 100%; (x) EtOH, toluene, reflux, 10 h, 71%; (xi) $Mn(OAc)_2{\cdot}4H_2O$, LiCl, EtOH, $CHCl_3$, reflux in air, 2 h, 94%.

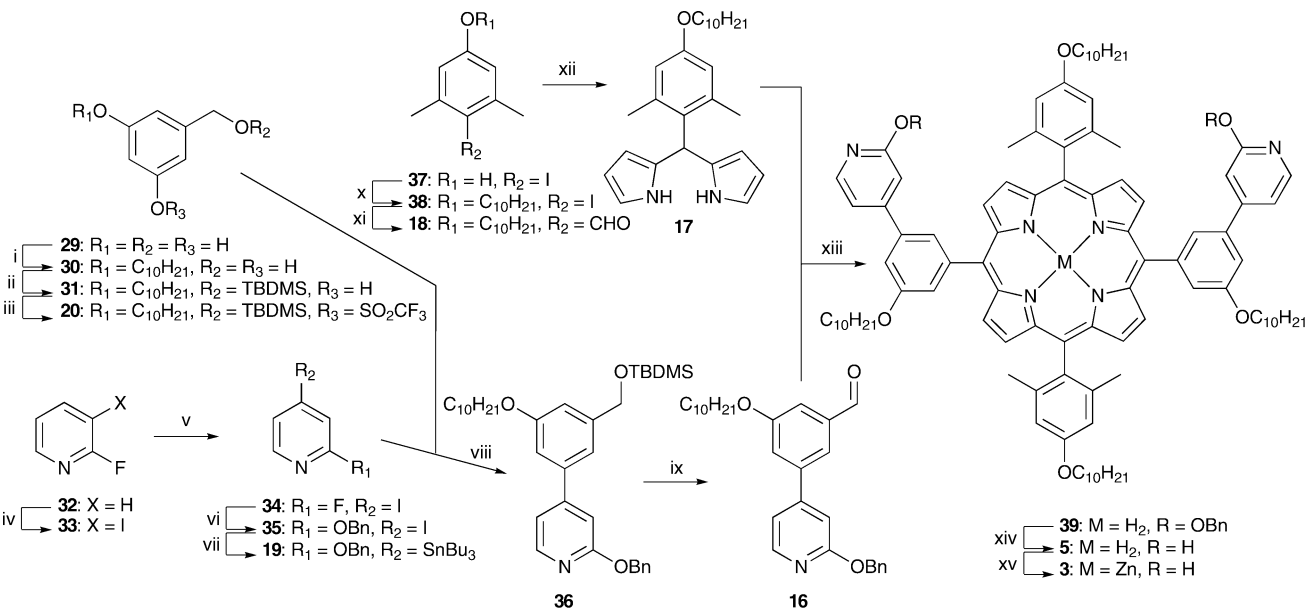

Scheme 5 Synthesis of Zn(porphyrin) **3** (i) 0.33 equiv. $C_{10}H_{21}Br$, K_2CO_3, 18-crown-6, acetone, reflux, 24 h, 66% (from $C_{10}H_{21}Br$); (ii) TBDMSCl, imidazole, DMF, rt, 12 h, 99%; (iii) Tf_2O, pyridine, rt, 17 h, 75%; (iv) LDA, THF, −78 °C, 4 h, then I_2, THF, −78 °C, 1 h, 72%; (v) LDA, THF, −78 °C, 4 h, then H_2O, THF, −78 °C, 1 h, 98%; (vi) BnOH, KOH, 18-crown-6, toluene, reflux, 3 h, 92%; (vii) *n*-BuLi, THF, −78 °C, 4 h, then Bu_3SnCl, THF, rt, 1 h, 96%; (viii) $Pd(PPh_3)_4$, LiCl, DMF, 90 °C, 48 h, 47%; (ix) DDQ, CH_2Cl_2, rt, 24 h, 85%; (x) $C_{10}H_{21}Br$, K_2CO_3, acetone, reflux, 24 h, quant; (xi) *n*-BuLi, THF, −78 °C, 1.5 h, then DMF, THF, rt, 85%; (xii) 25 equiv. pyrrole, TFA, rt, 1 h, 16%; (xiii) TFA, CH_2Cl_2, rt, 3 h, then DDQ, CH_2Cl_2, rt, 1 h, 23%; (xiv) TFA, PhSMe, rt, 24 h, quant; (xv) $Zn(OAc)_2$, $CHCl_3$, MeOH, reflux, 1 h, quant.

toluene. Subsequent iodine–lithium exchange, quenching the aryllithium intermediate with Bu_3SnCl, afforded stannylated pyridine **19**, a Stille coupling partner, in 96% yield. The other coupling partner, *meta*-phenylene spacer module **20**, was prepared in three steps from 3,5-dihydroxybenzyl alcohol (**29**, Scheme 5). After some experimentation, the following order of functionalisation was found to be optimal: monoalkylation with 0.33 eq of bromodecane and K_2CO_3 in refluxing acetone afforded phenol **30** in 66% yield from bromodecane. Compound **30** was easily separated from the unreacted excess of **29** by trituration of the crude product with chloroform. Approximately 70% of unreacted **29** could be recovered and reused. Phenol **30** was selectively silylated at the

benzyl alcohol position with TBDMSCl and imidazole in DMF, followed by triflation of the remaining phenol hydroxy group using Tf_2O in pyridine, giving **20** in 75% yield over two steps. Now, the Stille cross-coupling could be carried out on partners **19** and **20**, using $Pd(PPh_3)_4$ and LiCl in DMF, to obtain biaryl **36** in 47% yield. The silyl group was then oxidatively removed using DDQ,[18] affording aldehyde **16** in 85% yield.

For the nonstatistical synthesis of a *trans*-A_2B_2 porphyrin such as **3**, a dipyrromethane is required to react with aldehyde **16** in a [2 + 2] cyclocondensation. Dipyrromethane **17** was thus synthesised in three steps from iodophenol **37**, which in turn was prepared following a published procedure (Scheme 5).[19] Phenol **37** was quantitatively alkylated with bromodecane and K_2CO_3 in refluxing acetone yielding **38**, followed by iodine–lithium exchange, and subsequent quenching with DMF to obtain aldehyde **18** in 85% yield over two steps, after acidic aqueous workup. The dipyrromethane was then obtained following a method by Lindsey,[20] by mixing **18** with 25 equivalents of pyrrole and a catalytic amount of TFA. The purification involved both bulb-to-bulb distillation and recrystallisation. The long alkyl substituent created problems in both purification steps, requiring temperatures above 200 °C for the vacuum distillation of this heat sensitive compound and making it difficult to crystallise. As a result, dipyrromethane **17** could be isolated in only 16% yield. The subsequent porphyrin synthesis from **16** and **17** was carried out under Lindsey conditions; in dilute dichloromethane solution with a catalytic amount of TFA, followed by DDQ oxidation,[21] giving porphyrin **39** in 23% yield. The benzyl groups were removed by thioanisole in TFA in quantitative yield, liberating the 2-pyridone hydrogen-bonding motifs. Finally, treatment of porphyrin **5** with $Zn(OAc)_2{\cdot}2H_2O$ in a refluxing chloroform–methanol 9 : 1 mixture provided quantitatively the receptor porphyrin **3**.

After initial difficulties following the classical Lindlar type alkyne hydrogenation route in the synthesis of substrates **6**–**8**, we turned our focus to a rather uncommon transformation developed by H. C. Brown *et al.*: conversion of ketones to *Z*- or *E*-alkenes with complete stereoselectivity by hydroboration of the corresponding enamines, followed by controllable *anti* or *syn* elimination, respectively, of the amine–borane complex.[22] While the ketone required for substrate **6** was commercially available, those required for **7** and **8** were easily obtained by very similar two-step one-pot procedures (**40** and **41**, Scheme 6). The enamine intermediates (**43**–**45**) were efficiently prepared from ketones **40**–**42** using morpholine and titanium tetrachloride in benzene[23] (Scheme 7). Brown's hydroboration–elimination method using 9-BBN in THF followed by methanolysis provided the substrates **6**–**8**

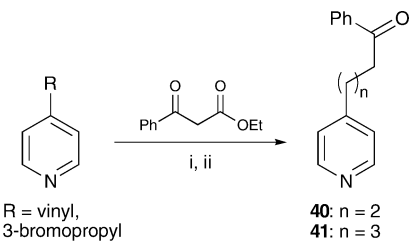

Scheme 6 Synthesis of presubstrate ketones **40** and **41**. (i) For R = vinyl, sodium, 180 °C, 4 h, or for R = 3-bromopropyl, sodium, EtOH, toluene, reflux, 4 h; (ii) 6 M HCl, reflux 6 h, 55% (n = 2, 2 steps), 31% (n = 3, 2 steps).

Table 1 Yields in the synthesis of olefinic substrates **6**–**8**

X[a]	n[a]	Enamine (yield)	Substrate (yield)
CH	2	**43** (94%)	**6** (65%)
N	2	**44** (80%)	**7** (38%)
N	3	**45** (90%)	**8** (52%)

[a] X and n refer to variable groups in structures in Scheme 7.

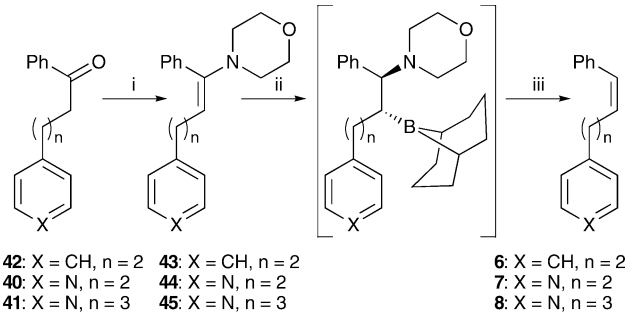

Scheme 7 Synthesis of olefin substrates **6**–**8**. (i) Morpholine, $TiCl_4$, benzene, rt, 24 h; (ii) 9-BBN, THF, rt, 3 h (iii) MeOH, rt, 2 min. For yields refer to Table 1.

with complete stereospecificity in moderate yields (see Table 1). Two equivalents of 9-BBN had to be employed for pyridine containing enamines, and the formed borane–pyridine complex imposed some difficulty in the workup, contributing to the diminished yields in those cases.

The long, rigid pyridine *N*-oxide derivative (**12**) was easily obtained in two steps from 4-bromopyridine and 4-*tert*-butylphenylboronic acid (Scheme 8). First, a Suzuki cross-coupling in a refluxing two-phase toluene–water mixture gave arylpyridine **46** in 80% yield, which was then catalytically oxidised using methyltrioxorhenium (MTO) and hydrogen peroxide,[24] affording *N*-oxide **12** in 74% yield after recrystallisation from a hexane–benzene mixture.

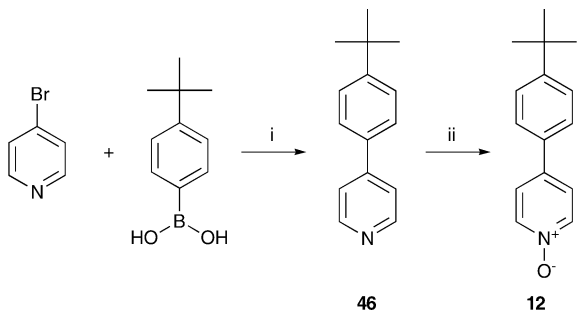

Scheme 8 Synthesis of the long, rigid pyridine *N*-oxide derivative **12**. (i) $Pd(PPh_3)_4$, Na_2CO_3, benzene, H_2O, reflux, 16 h, 80%; (ii) 30% aq. H_2O_2, MTO, CH_2Cl_2, rt, 24 h, 74%.

A complete association model for system 2 + 3

In order to relate the observed trends in substrate- and enantioselectivity at varying temperatures and concentrations of **2** and **3** to the proportion of catalyst **2** as macrocycle **1**, knowledge of the association constant for the formation of **1** from **2** and **3** is required. A rough estimate of 2×10^3 M^{-1} in dichloromethane at

298 K for the association constant had previously been obtained from the above selectivity studies, neglecting the possibility of linear oligomeric species in solution.[4] The results from following association analyses based on NMR and VPO experiments did not support the idea of dimerisation being the major form of association. Dilution experiments of a 1 : 1 mixture of metal free salen and porphyrin ligands **4** and **5** in deuterochloroform, performed using a 500 MHz NMR spectrometer, revealed the presence of not one or two, but *three* pyridone NH resonances, one originating from **4** and two from **5**. In the NMR spectrum of porphyrin **5**, all proton resonances were duplicated except for the ones from the benzylic methyl groups of the aromatic substituents in positions 10 and 20 on the porphyrin ring in **5**, which appeared as three singlets. This suggested the presence of two slowly interchanging, but unisolable conformers of porphyrin **5**, *cisoid* (**5c**) and *transoid* (**5t**). Since the concentration dependence of the two NH resonances from porphyrin **5** was not the same, it was concluded that the *cisoid* conformer was engaged in the assembly of a discrete macrocyclic oligomer. Following up on this conclusion, molecular modelling revealed that a macrocyclic trimer of porphyrins **3** or **5** can easily be formed without requiring the porphyrin units to adopt any strained conformations (Fig. 3). Thus it was clear that the set of equilibria involved in supramolecular system **2** + **3** is much more complex than expected. Not only does that make the equilibrium system more difficult to solve, but also more difficult to judge what assumptions and simplifications are reasonable to suggest in order to make its solution more manageable. We found ourselves forced to define a complete association model for system **2** + **3** without any assumptions or simplifications (see Fig. 4). The model is basically an extension of the so called equal K (K_E) model for indefinite self-association,[25] to include copolymerisation, as well as formation of the relevant macrocyclic structures. It includes six equilibria: the self-association of **2** (K_{22}), the self-association of **3** (K_{33}), the association of **2** with **3** (K_{23}), the formation of macrocycle **1** from a linear **2**–**3** dimer (K_1), the formation of macrocyclic trimer $\mathbf{3}_{3MC}$ from a linear trimer of **3** (K_T) and the *cisoid*–*transoid* conformational equilibrium of **3** (K_i). The assumption that the association strength in the addition of one monomer to the end of a polymer is independent of the length of the polymer is valid in nonpolar solvents where solvent interactions are minimal. The mathematical expression of this model requires the stringent use of linear algebra and is presented in detail elsewhere.[26] The general form of this model can in principle be applied to the association analysis of linear supramolecular copolymers of any number of components, involving specific terms for important macrocyclisations. It allows independent estimation of the strength of association for each pair of component types, and the calculation of the concentration of specific oligomers of any composition. Such an expression describing supramolecular copolymerisation based on a self-complementary recognition motif as in the present case has not appeared in the literature to date.

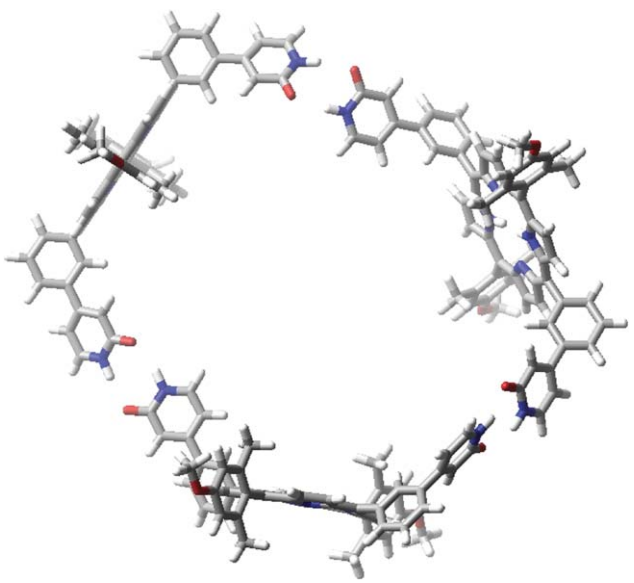

Fig. 3 A molecular mechanics[9] 3D representation of the hydrogen-bonded macrocyclic porphyrin trimer $\mathbf{3}_{3MC}$.

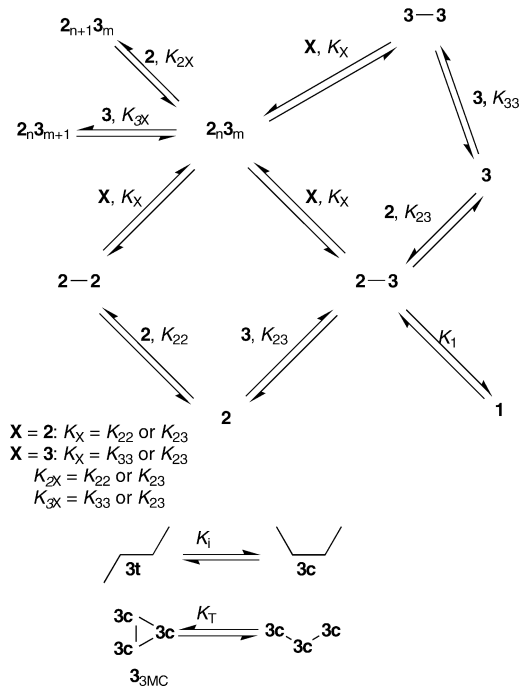

Fig. 4 The full equilibrium scheme of the complete association model for system **2** + **3**: the curved double arrow represents the elongation or shortening of a $\mathbf{2}_n\mathbf{3}_m$ polymer by one unit of **2** or **3** by addition to or elimination from the polymer, as governed by the relevant equilibrium constant K_x.

Curve fitting to such a complex model requires a large amount of experimental data. Roughly 300 data points of the chemical shift of the NH proton resonances were obtained in extensive variable temperature NMR dilution experiments in deuterochloroform of salen ligand **4**, porphyrin **5** and a 1 : 1 mixture of the two. Instead of fitting the variation of observed chemical shifts with concentration at each temperature, all observed chemical shifts at different temperatures were fitted simultaneously to obtain the $\Delta H°$ and $\Delta S°$ values for each of the six equilibria, producing a globally best fit. These values are shown in Table 2 along with the equilibrium constant values derived from the thermodynamic parameters at various temperatures. The fitting of the NMR data was done using the program Matlab. A detailed algorithm for the optimisation of the different parameters will be described

Table 2 Thermodynamic parameters and derived association constants at various temperatures in $CDCl_3$ for the six different equilibria of the complete association model for system **2** + **3**[a]

T/K	$10^{-2} \times K_{22}$/M^{-1} [b]	$10^{-3} \times K_{33}$/M^{-1} [b]	$10^{-2} \times K_{23}$/M^{-1} [b]	K_1 [b]	K_T [b]	K_i [b]
233	44.8(38.7, 51.8)	78.2(67.3, 90.7)	25.9(13.5, 49.7)	246.0(149.3, 405.6)	91.6(57.2, 146.6)	1.7 (1.2, 2,4)
263	8.2(7.4, 9.1)	12.1(11.0, 13.3)	9.0(6.1, 13.3)	59.9(46.1, 77.8)	38.1(29.3, 49.4)	1.3 (1.1, 1.5)
273	5.0(4.6, 5.6)	7.1(6.5, 7.7)	6.7(4.9, 9.3)	40.0(32.5, 49.4)	29.6(24.0, 36.6)	1.2 (1.1, 1.3)
283	3.2(2.9, 3.5)	4.3(4.0, 4.7)	5.1(3.9, 6.7)	27.6(23.1, 32.9)	23.5(19.8, 27.9)	1.1 (1.0, 1.2)
298	1.7(1.6, 1.9)	2.2(2.0, 2.4)	3.5(2.8, 4.3)	16.5(13.9, 19.6)	17.1(14.7, 19.8)	1.0 (0.9, 1,1)
313	1.0(0.9, 1.1)	1.2(1.1, 1.3)	2.5(2.0, 3.0)	10.4(8.4, 12.8)	12.8(10.9, 15.1)	0.9 (0.8, 1.0)
$\Delta H°$/kJ mol^{-1}	−28.8 ±0.5	−31.7 ±0.7	−17.8 ±2.5	−24.0 ±2.3	−14.9 ±2.0	−4.8 ± 1.7
$\Delta S°$/J mol^{-1} K^{-1}	−53.9 ±1.8	−42.3 ±2.4	−11.3 ±8.1	−57.2 ±7.9	−26.4 ±6.6	−16.1 ± 5.9

[a] The complete model and the equlilbria involved are shown in Fig. 4. For mathematical expression of the model and estimation of values of association constants, see ref. 26. [b] 95% confidence interval (min, max). See ref. 26 for computational details.

Table 3 Observed selectivity of system **2** + **3** for the competitive epoxidations of **7** *vs* **6** in deuterochloroform at different temperature and the respective mole fraction of **2** in the different states (*a*, *b*, *c* and *d*)[a]

T/K	Sel **7** *vs* **6**	χ_a[a]	χ_b[a]	χ_c[a]	χ_d[a]
213	1.42	0.032 ± 0.001	0.669 ± 0.026	0.164 ± 0.026	0.136 ± 0.010
263	1.46	0.115 ± 0.002	0.460 ± 0.012	0.225 ± 0.015	0.201 ± 0.006
273	1.52	0.155 ± 0.002	0.398 ± 0.008	0.241 ± 0.011	0.206 ± 0.004
283	1.55	0.200 ± 0.002	0.340 ± 0.006	0.256 ± 0.009	0.203 ± 0.004
298	1.38	0.271 ± 0.003	0.266 ± 0.006	0.276 ± 0.011	0.187 ± 0.005
313	1.38	0.341 ± 0.007	0.205 ± 0.007	0.291 ± 0.017	0.162 ± 0.007

[a] The mole fraction of **2** in its different supramolecular states (*a*, *b*, *c* and *d*, see Fig. 5) at $[\mathbf{2}]_{tot} = [\mathbf{3}]_{tot} = 5.0$ mM. See ref. 26 for computational details.

elsewhere.[26] Using these results, the molar fractions of the different species could be calculated and will be used in the extensive analysis of catalytic experimental results further on (*vide infra*), with the assumption that **4** and **5** accurately represent the solution behaviour of the corresponding metal complexes **2** and **3** in terms of hydrogen-bond based associations. The results of this careful analysis strongly contrast the previous assumption that macrocycle **1** is the major catalytic species in solution. In fact, it never exceeds 20% under normal reaction conditions (see column χ_d in Table 3). The previous estimation of the inherent substrate selectivity of macrocycle **1**[4] is thereby obsolete and should be reconsidered with respect to this complete association model.

Aspects on the mechanism of the Jacobsen–Katsuki epoxidation. Implication for the supramolecular system 2 + 3

The J–K epoxidation can partly proceed *via* a radical pathway, rationalising the observation of products from epimerisation,[28] but the stereospecific epoxidation presumably takes place *via* a concerted addition.[29] Multiple potential oxidants are present in the reaction mixture, but it is currently a matter of dispute which of these species are responsible for the oxygen transfer to the olefin.[30] In lack of a general consensus on the matter, we are forced to define our own view, based on the available literature information, to keep a consistent background to the analysis of our results. The O=Mn(V)(salen) species, the originally proposed catalytic oxidant in Mn(salen) catalysed epoxidations,[31] is still believed to be important. Recently, however, alternative catalytic oxidants have been proposed in multiple competing reaction pathways, to explain the profound effects that the nature of the stoichiometric oxidant, catalyst counter ion and added donor ligands exert on catalyst reactivity, stability, stereo- and enantioselectivity.[32,33] However, we propose that there is no need to invoke any alternatives to O=Mn(V)(salen) to explain these effects. The O=Mn(V)(salen) species has one vacant coordination site. Due to its instability, it has been impossible to estimate the coordination properties of this site. The donor ligands typically employed in the J–K epoxidation *i.e.* imidazole, pyridine and pyridine *N*-oxide derivatives, coordinate much too weakly to Mn(III)(salen)[34] to possibly account for the effects they have on the course of the reaction, indicating that the O=Mn(V)(salen) species has a much higher affinity for axial coordination than Mn(III)(salen) has.[35] Donor ligands and even PhIO have been shown by mass spectrometric (MS) studies to coordinate to O=Mn(V)(salen), inducing the formation of μ-oxo dimers.[36] Given this relatively strong affinity, we can propose that all potential ligand functionalities in a particular reaction mixture continuously compete for axial coordination to O=Mn(V)(salen). These ligands would include the catalyst counter ion, any added donor ligands (imidazoles, pyridines, *N*-oxides), and stoichiometric oxidant (PhIO, OCl^-, mCPBA), heteroatom-containing functional groups in substrate molecules and even in the epoxide product. Therefore, the active catalytic oxidant is O=Mn(V)L(salen) where each ligand L gives the oxidative Mn complex distinct characteristics, dictated by the nature of L, in terms of reactivity in epoxidation, stability towards inactivation, stereoselectivity, and enantioselectivity. The relative proportions of the various O=Mn(V)L(salen) species are determined by the concentrations and coordination strength of the different L ligands. If L is the stoichiometric oxidant, a catalytic cycle without a Mn(III) intermediate might be possible.[37] The result of the reaction can be made independent of the oxidant employed by adding the strongly coordinating[34] 1-methylimidazole ligand.[33] It has long been known that beyond a certain concentration, the beneficial effects of a donor ligand

additive are reversed, and the stability of the catalyst plummets above this concentration.[31] The inactivation of the catalyst in the J–K epoxidation has typically been ascribed to the formation of a catalytically inactive μ-oxo dimer.[38] However, the μ-oxo dimer species that have been proposed[31] and observed by MS[36] were formed from unsubstituted, achiral Mn(salen) complexes. No μ-oxo dimers were observed in identical MS experiments using the more sterically congested Jacobsen's catalyst.[39] The competitive coordination hypothesis presented above could explain these donor ligand effects without the involvement of μ-oxo dimers. Too strongly coordinating donor ligands might outcompete the stoichiometric oxidant in the coordination to reduced Mn(salen) species, retarding reoxidation to O=Mn(V)(salen).

The consequences of our competitive coordination hypothesis in supramolecular system **2** + **3** can be derived by considering Fig. 5, which shows schematically the four possible supramolecular states of catalyst **2**. In the absence of receptor **3**, catalyst **2** can exist in state *a* or *b*, as a free monomer or as a member of a linear hydrogen-bonded $\mathbf{2}_n\mathbf{3}_m$ oligomer with only **2** as a next hydrogen-bonded neighbour, respectively. States *a* and *b* of the oligomers $\mathbf{2}_n\mathbf{3}_m$ were shown not to exhibit any substrate selectivity in the competitive J–K epoxidation of **7** *vs* **6**, since two reactions run in the absence of **3**, one at $[\mathbf{2}]_{tot} = 0.5$ mM (mainly monomers) and the other at $[\mathbf{2}]_{tot} = 5$ mM (mainly oligomers), showed the same product distribution. Upon addition of **3**, a considerable amount of **2** is shifted to states *c* and *d*, constituting a member of $\mathbf{2}_n\mathbf{3}_m$ oligomers with receptor **3** as a next hydrogen-bonded neighbour and the hydrogen-bonded macrocyclic dimer **1**, respectively (see columns χ_c and χ_d in Table 3). Although much more flexible, the oligomeric state *c* can be expected to show many of the properties of the macrocyclic state *d* in terms of catalytic behaviour and selectivity,

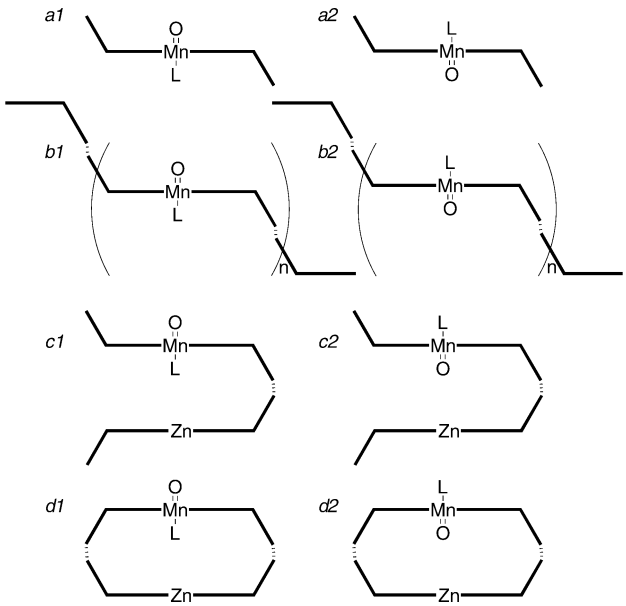

Fig. 5 The four possible supramolecular states of catalyst **2** in solution. State *a*: as a free monomer. State *b*: as a part of a linear hydrogen-bonded $\mathbf{2}_n\mathbf{3}_m$ polymer with only **2** as next hydrogen-bonded neighbours. State *c*: as a part of a $\mathbf{2}_n\mathbf{3}_m$ polymer with receptor **3** as a next hydrogen-bonded neighbour. State *d*: as the macrocyclic heterodimer **1**. In states *a* and *b*, both faces of the salen ligand in **2** are equivalent, while in *c* and *d* they are not.

due to the spatial proximity of the Zn centre of a receptor and a catalytic Mn centre in state *c*. Although the proportion of states *b* and *c* has previously been considered to be negligible in system **2** + **3**,[4] the complete association model suggests that both states *a* and *b* are in general populated to a similar extent as the expected selective states *c* and *d* (*vide infra* and Table 3). In states *a* and *b*, both faces of the Mn(III)(salen) complex are identical, and oxidation of Mn at either face leads to equivalent O=Mn(V)L(salen) species *a1* and *a2* or *b1* and *b2*. Thus, the distribution of axial ligands L will be the same in both species, and all substrates which may be present in the reaction mixture will experience the same distribution of catalytic oxidants. In contrast, oxidation of Mn in states *c* and *d* introduces a differentiation of the catalyst faces to an *endo* face and an *exo* face. The two faces are not equally accessible to axial ligands, which may lead to 1) unequal proportions of *c1* and *c2* (and *d1* and *d2*) if the two faces are not equally accessible to the stoichiometric oxidant, and 2) different distributions of axial ligands L in *c1* and *c2* (and in *d1* and *d2*) if for example, some L cannot easily be accommodated within the space between the Mn and Zn metal centres. If one component of a substrate mixture is preferably bound and epoxidised inside the cavity of states *c* or *d* while another is not accommodated inside and is therefore preferably epoxidised by the *exo* face of the catalyst, the stereo- and enantiomerical distribution in the two corresponding epoxide products will therefore appear as if they were produced by two distinct catalysts. We tried to turn this complication to our favour, by using the long *N*-oxide ligand **12**, not accommodated inside the cavity of **1**, to shift the proportions of *c1* and *c2* (*d1* and *d2*) towards *c2* (*d2*). However this attempt did not appear to be successful, as previously reported.[4]

The effect of various reaction components on the stability, reactivity and substrate selectivity of catalyst 2

Twelve epoxidation reactions using catalyst **2** were carried out at 24 °C in dichloromethane and monitored by GC, following the consumption of olefinic substrates. All the reactions were 5.0 mM in **2** and 100 mM in substrate (in competition reactions, 50 mM of each substrate). 1.2 equivalents of the oxidant iodosylbenzene (PhIO) were employed. Two substrates, **6** and **7** were used, both in competition and separate epoxidations (Scheme 1). The composition of the reaction mixtures was systematically varied in terms of the presence of substrates **6** and **7**, *N*-oxide ligand **12** (20 mM) and porphyrin receptor **3** (5.0 mM) (see Table 4). From the time curves obtained from the GC data, the reactivity and stability of catalyst **2** can be compared as a function of the composition of the reaction mixture, and the isolated effects of each component can be evaluated. Table 4 shows the reactivity of **2**, expressed as the observed initial first order rate constants (k_{obs}) for the consumption of each substrate and also of total substrate in competition reactions. The values for k_{obs} are obtained from the observed conversions at the first data point ($t = 60$ s) using the rate law: $rate = k$[O=Mn(V)(salen)][substrate] with the assumption that catalyst concentration is constant, giving $rate = k_{obs}$[substrate].[27] Table 4 also shows the isolated effect of each reaction component as the ratio of rate constants with and without the particular component with other variables unchanged. The effects on catalyst **2** of receptor **3**, by hydrogen-bonding with catalyst **2**, as well as *N*-oxide **12** and the pyridine moiety of substrate **7**, by coordination to

Table 4 Reaction scheme, observed initial rate constants and isolated component effects on catalyst reactivity in the epoxidation of substrates **6** and **7** by catalyst **2** in the presence or absence of various reaction components[a]

Entry	**3**	**12**	**7**	**6**	$10^3 \times k_{obs}$(**7**) (s^{-1})[b]	$10^3 \times k_{obs}$(**6**) (s^{-1})[b]	$10^3 \times k_{obs}$(**6** + **7**) (s^{-1})[b]	Effect of **3**[c,d]	Effect of **12**[c,e]	Effect of **7**[c,f]
1	×	×	×	×	2.8	1.9	2.3	0.49	1.00	0.74
2	×	×	×		2.3		2.3	0.47	0.96	0.74
3	×	×		×		3.1	3.1	0.74	0.89	
4	×		×	×	3.1	1.6	2.3	0.66		0.66
5	×		×		2.4		2.4	0.49		0.69
6	×			×		3.5	3.5	0.97		
7		×	×	×	3.9	5.3	4.7		1.34	1.12
8		×	×		4.9		4.9		1.00	1.17
9		×		×		4.2	4.2		1.17	
10			×	×	2.4	4.6	3.5			0.97
11			×		4.9		4.9			1.36
12				×		3.6	3.6			

[a] Reaction conditions: solvent: CH_2Cl_2, $T = 24$ °C, $[\mathbf{2}]_{tot} = 5.0$ mM, $[\mathbf{6}]_{tot} + [\mathbf{7}]_{tot} = 100$ mM, mixtures of **6** and **7** are always 1 : 1, 1.2 equiv. PhIO, $[\mathbf{3}]_{tot} = 5.0$ mM or 0, $[\mathbf{12}]_{tot} = 20$ mM or 0. [b] Estimated from the conversion at $t = 60$ s. [c] Calculated using k_{obs}(**6** + **7**) values. [d] k_{obs}(entry n)/k_{obs}(entry $n + 6$). [e] k_{obs}(entry n)/k_{obs}(entry $n + 3$). [f] k_{obs}(entry n)/k_{obs}(entry $n + 2$), then k_{obs}(entry n)/k_{obs}(entry $n + 1$).

Mn, were systematically investigated as described above (Table 4). We have been cautious in our conclusions because the differences in the values of k_{obs} are quite small and the number of data points is limited. Examination of the epoxidation rates of the reactions with nonbinding substrate **6** only (entries 3, 6, 9 and 12), suggests that receptor **3** changes the steric environment around the Mn center, probably by forming supramolecular states *c* and *d* by hydrogen-bonding, and thus modulating the availability of Mn for interaction with coordinating ligands but allowing the substrate to be oxidised anyway from the *exo*- and *endo* face. On the other hand, the epoxidation rates of the reactions with substrate **7** only (entries 2, 5, 8 an 11), can be interpreted as if the reaction is taking place mainly on the *endo* face of the catalyst when **7** is coordinated to the zinc of receptor **3** and that binding or releasing of either substrate **7** or product **10** is the rate-limiting step in the catalysis. By comparing the competition experiments with single substrate experiments, we can see more intriguing facts. The epoxidation rates in the absence of receptor **3** (entries 7–12) indicate that both pyridine substrate **7** and *N*-oxide **12** act as donor ligands and activate the catalyst for substrate **6**. This activation is even more pronounced when both substrate **7** and *N*-oxide **12** are present. However in the presence of **3**, the addition of **7** dramatically decreases the reactivity of the catalyst for **6**, no matter whether **12** is present or not (entry 1 *vs* 3 and 4 *vs* 6). Thus, it seems that receptor **3** cancels the effect of **12**. On the other hand in the presence of **3**, the addition of **6** increases the reactivity for **7** no matter whether **12** is present or not (entry 1 *vs* 2 and 4 *vs* 5). Another interesting point for the competition experiments in the presence of **3** is that the addition of **7** decreases the overall reactivity of catalyst **2**, expressed as k_{obs}(**6** + **7**) no matter whether **12** is present or not (entry 1 *vs* 3 and 4 *vs* 6). This behaviour is quite similar to when only **7** is present (entry 1 *vs* 2 and 4 *vs* 5). It appears as **7** slows down any reaction in the presence of **3** but does not have this effect on the epoxidations performed without **3** (entries 7–12). This can be interpreted so as there is always at any time a pyridine-containing substance (substrate **7** or product **10**) coordinated to receptor **3**, forcing substrate **6** to be epoxidised on the *exo* face while **7** can react on both faces. This also indicates that the binding or releasing of substrate **7** or product **10**, respectively, might be the over-all rate-limiting step.

The kinetics and substrate selectivity profiles for the twelve reactions in Table 4 are shown in Fig. 6, where results from the competition experiments between pyridine-containing receptor-binding substrate **7** and nonbinding substrate **6** are illustrated in Fig. 6a–b, while single substrate experiments using **6** or **7** appear in Fig. 6c–d, respectively. We can see from Fig. 6a and c–d that the presence of receptor **3** stabilises the catalyst **2** as much as the presence of *N*-oxide **12** does. However in the absence of substrate **7**, this stabilisation is even more pronounced (Fig. 6d).

The substrate-selectivity profiles in Fig. 6b show some interesting features. First they suggest that substrate **6** is at least twice as reactive than **7** when the two substrates are in competition, in the absence of receptor **3** no matter whether **12** is present or not (entry 7 and 10), see also the same entries in Table 4). Second, the relative selectivity[4] of catalytic system **2** + **3** for substrate **7** over **6**, normalised to the corresponding selectivity of catalyst **2**, can be estimated to 1.68 at approximately 24% conversion, as compared to the previously more rigorously calculated value of 1.48 ± 0.14 at 20% conversion.[4] The curve corresponding to entry 4, representing receptor **3** without *N*-oxide **12**, is the most interesting one. At the lowest conversion (13%), the absolute selectivity (conv(**7**)/conv(**6**)) is much higher than with **12** present (entry 1), almost reaching a value of 2. But as the conversion increases, the selectivity decreases to a level similar to that of entry 1, and the two curves closely follow each other at conversions above 25%. This is an indication of product inhibition. In the beginning of the reaction, catalyst **2** in direct hydrogen-bonded contact with receptor **3** (states *c* and *d*), is available for epoxidation of receptor-binding substrate **7** at the *endo* face, but as soon as the concentration of epoxide **10** builds up, it increasingly occupies the cavity between the Mn and Zn metal centres with the aid of a two point interaction: The pyridine coordinates to Zn, as it should, and thereby preorganises the epoxide oxygen, normally a weak and noncompetitive ligand, to coordinate to Mn. Thus, states *c* and *d* may form somewhat more stable complexes with epoxide **10** than with substrate **7**. In this scenario, continuing epoxidation is forced to occur to a higher degree on the *exo* face of the catalyst and thus decreasing the substrate selectivity of system **2** + **3**. The fact that this higher selectivity is not observed at low conversion under standard conditions in the presence of *N*-oxide **12** suggests

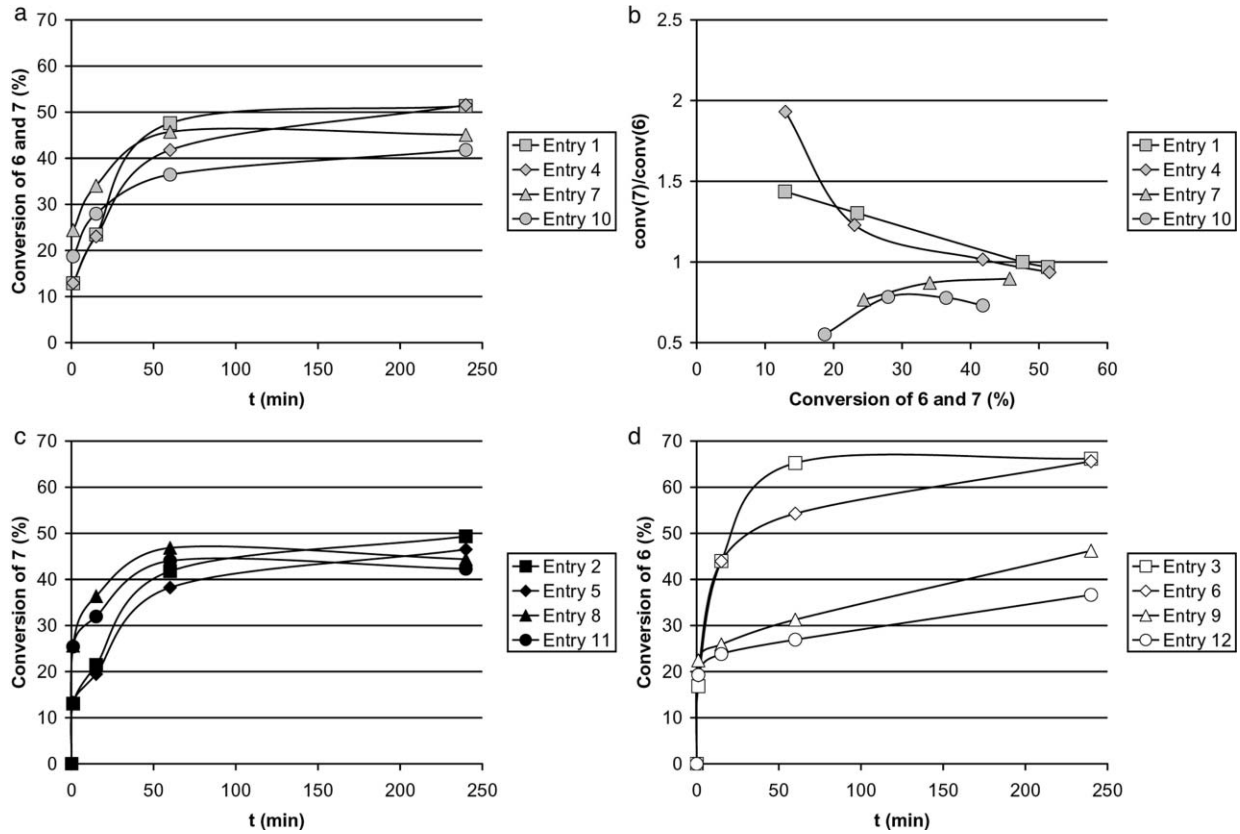

Fig. 6 Kinetic and selectivity profiles for the epoxidation of substrates **6** and **7** with catalyst **2** under standard conditions in the presence of both receptor **3** and *N*-oxide ligand **12** (□), **3** only (◇), **12** only (△) or none of the two (○). Entry numbers refer to Table 4. (a) Total olefin conversion in competition experiments (**7** *vs* **6**, grey filled markers); (b) substrate selectivity (**7**/**6**) in competition experiments; (c) conversion of **7** in single substrate reactions (black filled markers); (d) conversion of **6** in single substrate reactions (empty markers).

that **12** actually blocks the cavity from the beginning, or partly inhibits the hydrogen-bonded formation of states *c* and *d*.

The stability of catalysts is typically expressed as turnover number (TON). This value is often measured with lower catalyst loadings than is practical for preparative purposes, which compromises the yield but maximises the TON value. To increase the comparative value of TON for different catalysts, common substrates are generally used, underlining that an observed difference between two systems originates from the catalysts and not the substrates. We thus performed epoxidations with styrene, a very common substrate in J–K epoxidations and 0.2% catalyst loading to estimate the TON of catalyst **2**. Six experiments with varying combinations of receptor **3** (4.0 mM), *N*-oxide **12** (4.0 mM) and 4-ethylpyridine (**47**, 0.10 M) were carried out. The reactions were run at 24 °C in dichloromethane with PhIO as the stoichiometric oxidant and were 0.50 M in styrene and 1.0 mM in catalyst **2**. Four equivalents of receptor **3** were employed to ensure the formation of the two substrate selective catalyst states (*c* and *d*), to a large extent at this low concentration of **2**. Under these conditions the mole fraction of **2** in the different states in Fig. 5 is $\chi_a = 0.357 \pm 0.006$, $\chi_b = 0.065 \pm 0.002$, $\chi_c = 0.285 \pm 0.011$ and $\chi_d = 0.293 \pm 0.007$.[26] Pyridine **47** was chosen to emulate the coordinating pyridine moiety of substrate **7** because it was expected to have similar electron density as **7** on the pyridine ring and hence, similar coordination strength and effects on the catalytic behaviour of **2**. The reaction scheme and TONs obtained after 5 h of reaction are shown in Table 5. Extending the time to several days might increase the TON by 5% in some cases and by 20% in others, but the general trend would be the same. In the absence of **47**, the TONs are around 150 (entries 2 and 5). In the presence of **47** however, the TONs group around 50–60. A slight stabilising effect of receptor **3** can be discerned. These observations are similar to those obtained from the kinetic profiles for substrate **6** in Fig. 6d.

Table 5 TON of catalyst **2** in the presence or absence of additives

Entry	**3**	**12**	**47**	TON[a]
1	×	×	×	60
2	×	×		162
3	×		×	55
4		×	×	52
5		×		149
6			×	52

[a] Determined after 5 h of reaction at 24 °C and 0.2% catalyst loading, using styrene as substrate in dichloromethane.

Temperature effects on substrate- and enantioselectivity

One of the means to increase selectivity in a reaction is to run it at low temperature, thus increasing the enthalpic contribution to the free energy of the reaction and hence to the formation of the major product. In the case of system **2** + **3**, additional factors

may affect the temperature dependence of substrate selectivity: both the proportion of catalyst **2** in states *c* and *d* (Fig. 5) and the rates of assembly and substrate binding processes are temperature dependent.

For these reasons we were interested to see how much the substrate selectivity of system **2** + **3** could be improved by lowering the temperature. With this aim, we carried out competitive epoxidation reactions of substrates **7** *vs* **6** at six different temperatures (Scheme 1), measuring by GC and NMR the relative consumption of the two substrates and formation of the corresponding *cis*-epoxides (**10** and **9**, respectively) at 20% conversion. The conditions were the same as in previous competitive epoxidations, except that deuterated chloroform was used as the solvent to be able to relate the selectivity to the association constants obtained by the complete association model.[26] The results are shown in Fig. 7. Interestingly, there is not a clear trend of increasing selectivity with lower temperature. Instead, the selectivity is relatively constant over the temperature range (233–313 K). This can be qualitatively explained by the variation of the mole fractions of the different states of catalyst **2** with temperature. For the two states that can be expected to display selectivity, *c* and *d* (*vide infra*), both those two mole fractions decrease as the temperature decreases in this temperature range, *d* reaching a plateau at the higher temperatures. This becomes even more obvious if we look at the different competition reactions at 298 K with different concentration of **2** and **3** (Table 6). It is clear that heterodimer **1** is not the only substrate selective species in solution, since the selectivity at different conditions does not follow the same trend as the mole fraction of **2** in state *d*. However, taking in consideration both states *c* and *d*, we can see that the selectivity follows the same trend as for the mole fractions of **2** in state *c* + *d*. This is easier seen in Fig. 8. These observations are strong evidence that both states *c* and *d* are selective for **7**. Since it has been concluded from the kinetic studies that the reactivity of **2** decreases when **6** and **7** are epoxidised by system **2** + **3** and the exact mechanism of J–K epoxidation has never been established, it is not possible to quantify the inherent selectivity of the different states.

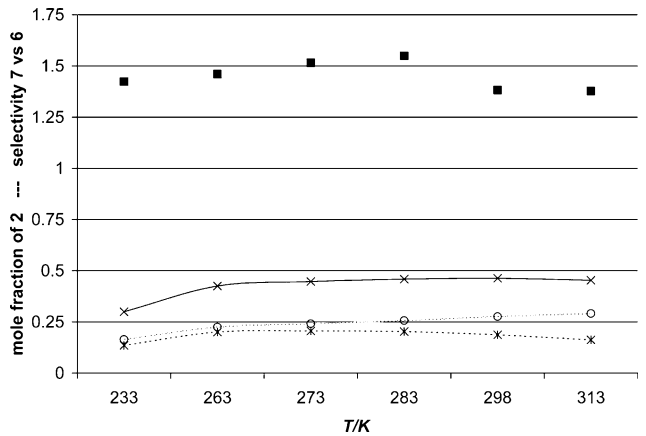

Fig. 7 Relative selectivity of system **2** + **3** in $CDCl_3$ for substrates **7** *vs.* **6** and mole fractions of the different states of catalyst **2** (responsible for substrate selectivity) as a function of temperature. The selectivity values are averages of substrate conversion ratios and product ratios as measured by GC and NMR, and are normalised to the simultaneously determined selectivity of catalyst **2**. Legend: measured selectivity (■), χ_c (○), χ_d (*), χ_{c+d} (×).

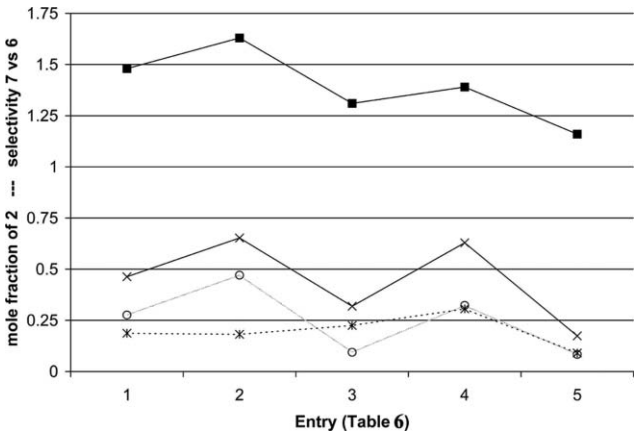

Fig. 8 Representation of the selectivity of the system **2** + **3** and the mole fraction of **2** in different states (*c*, *d* or *c* + *d*) at different concentrations of **2** and **3** at 298 K (entry 1–5, Table 6). Legend: measured selectivity (■), χ_c (○), χ_d (*), χ_{c+d} (×).

The enantioselectivities were determined by chiral GC to assess their temperature dependence, using either catalyst **2** or system **2** + **3** and either in competitive epoxidations of substrates **6** and **7** or with substrate **6** only. The measured enantiomeric excesses (ee) are given in Table 7 for the competitive epoxidations of substrates **6** and **7** and Table 8 for the single substrate epoxidation. There are two notable features in the observed ee data.

The first striking feature is that at all temperatures, the ee values of epoxide **10** (from substrate **7**) are lowered by approximately 30% when the reaction is run in the presence of receptor **3**, while this is not the case for epoxide **9** (from substrate **6**) neither in the presence of **7** (Table 7) nor in its absence (Table 8). Clearly, **3** changes the approach of substrate **7** to the Mn centre in a more direct and systematic way than of substrate **6**. To investigate the source of this behaviour, two experiments were performed. First, the epoxidation of **7** at 298 K without receptor **3** but in the presence

Table 6 Observed selectivity of system **2** + **3** at different concentrations of **2** and **3** at 298 K for the competitive epoxidations of **7** *vs* **6** in dichloromethane and the respective mole fraction of **2** in the different state (*a*, *b*, *c* and *d*)

Entry	$[2]_{tot}$/mM	$[3]_{tot}$/mM	sel **7**/**6**	χ_a[a]	χ_b[a]	χ_c[a]	χ_d[a]
1	5.0	5.0	1.48	0.271 ± 0.003	0.266 ± 0.006	0.276 ± 0.011	0.187 ± 0.005
2	5.0	15	1.63	0.192 ± 0.005	0.155 ± 0.006	0.471 ± 0.015	0.182 ± 0.006
3	0.5	0.5	1.31	0.607 ± 0.003	0.074 ± 0.001	0.094 ± 0.004	0.225 ± 0.004
4	0.5	5.0	1.39	0.342 ± 0.006	0.030 ± 0.001	0.323 ± 0.012	0.306 ± 0.007
5	5.0	1.0	1.16	0.366 ± 0.003	0.460 ± 0.004	0.084 ± 0.004	0.090 ± 0.002

[a] The mole fraction of **2** in its different supramolecular states (*a*, *b*, *c* and *d*, see Fig. 5) at $T = 298$ K in deuterochloroform.[26]

Table 7 Enantioselectivity of catalyst **2** with and without receptor **3**, and relative activation parameters for formation of the two enantiomers of each product **10** and **9** in competitive epoxidations of **7** and **6**[a]

	Epoxide **10** (from **7**)		Epoxide **9** (from **6**)	
T/K	ee cat. **2**	ee cat. **2** + **3**	ee cat. **2**	ee cat. **2** + **3**
263	73.0%	40.6%	63.0%	69.6%
273	72.3%	40.3%	65.7%	71.7%
283	74.6%	43.8%	68.6%	71.2%
298	80.2%	51.3%	73.5%	70.6%
313	78.3%	51.0%	68.9%	71.4%
$-\Delta\Delta H^{\ddagger}$/kJ mol^{-1}[b]	-4.8 ± 1.7	-4.4 ± 1.0	-3.8 ± 1.9	-0.5 ± 0.5
$\Delta\Delta S^{\ddagger}$/J mol^{-1} K^{-1})[b]	33 ± 6	24 ± 3	27 ± 7	17 ± 2

[a] Reaction conditions: solvent: $CDCl_3$, $[\mathbf{2}]_{tot} = 5.0$ mM, $[\mathbf{6}]_{tot} = [\mathbf{7}]_{tot} = 50$ mM, 0.2 equiv. PhIO, $[\mathbf{3}]_{tot} = 5.0$ mM or 0, $[\mathbf{12}]_{tot} = 20$ mM. [b] See Fig. 9.

Table 8 Enantioselectivity of catalyst **2** with and without receptor **3**, and relative activation parameters for formation of the two enantiomers of product **9** in single substrate epoxidations of **6**[a]

T (K)	ee Cat. **2**	ee Cat. **2** + **3**
263	79.2%	74.9%
273	78.4%	76.1%
283	78.3%	74.6%
298	76.4%	73.8%
303	75.5%	71.5%
313	73.5%	72.0%
$-\Delta\Delta H^{\ddagger}$ (kJ mol^{-1})	3.2 ± 9.4	2.6 ± 0.5
$\Delta\Delta S^{\ddagger}$ (J mol^{-1} K^{-1})	5.8 ± 1.4	6.9 ± 1.8

[a] Reaction conditions: solvent: $CDCl_3$, $[\mathbf{2}]_{tot} = 5.0$ mM, $[\mathbf{6}]_{tot} = 100$ mM, 0.2 equiv. PhIO, $[\mathbf{3}]_{tot} = 5.0$ mM or 0, $[\mathbf{12}]_{tot} = 20$ mM.

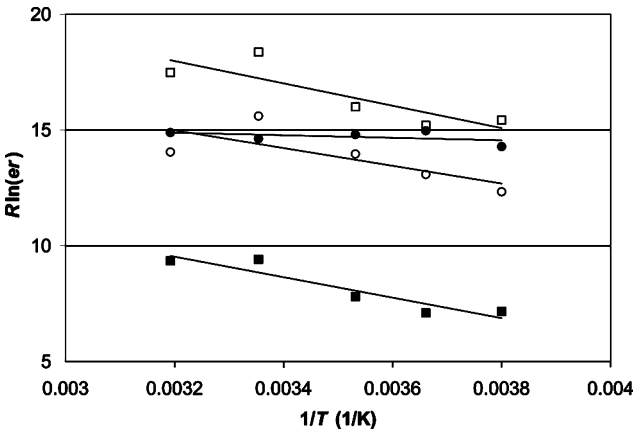

Fig. 9 Eyring plots for the enantiomeric ratio (er) expressed as Rln(er)in the competitive epoxidation of receptor-binding substrate **7** (■) and nonbinding substrate **6** (○) using catalyst **2** (empty markers) or catalytic system **2** + **3** (filled markers). The straight lines represent best least-square fits to observed data points in each series. The relative activation parameters and reaction conditions are given in Table 7.

of ZnTPP (5.0 mM) gave epoxide **10** in 78% ee, almost identical to that obtained without any porphyrin. Secondly, competition of the longer receptor-binding substrate **8** *vs* nonbinding substrate **6** at 298 K in the presence and absence of receptor **3** resulted in 63 and 59% ee of epoxide **11** (from substrate **8**), respectively. Thus, binding to receptor **3** does not have the same lowering effect on the ee of **11** as it does on **10**. From this it must be concluded that the receptor-binding substrates **7** and **8** are to a large extent epoxidised from the *endo* face of the catalyst in states *c* and *d*, while coordinated to receptor **3**, whereas nonbinding substrate **6** is not. The decrease in ee values observed only for **7** and not for **8** reflects the unfavourable approach of the olefin towards Mn in terms of enantioselectivity, enforced by binding to the receptor in supramolecular states *c* or *d* of catalyst **2**. The higher flexibility of the spacer between the binding- and reacting group in **8** allows the olefin to adopt a more optimal approach to the Mn centre while bound to the receptor, resulting in a higher ee of the epoxide **11** in the presence of **3**.

The second striking feature is that for both system **2** + **3** and **2**, the ee values increase with temperature when **6** and **7** are epoxidised in competition experiments (Table 7). On the other hand when **6** is the only substrate, the ee values decrease as one would expect from a normal reaction (Table 8). We analysed our data by drawing Eyring plots from the observed enantiomeric ratios (Fig. 9), using an Eyring selectivity equation[27] (eqn 1, er = enantiomeric ratio). Since there are potentially significant factors, not present in standard J–K epoxidations, influencing the ee in our system, Eyring plots such as those in Fig. 9 would not necessarily yield linear curves. Indeed, some of the data points in Fig. 9 deviate significantly from their least-square linear plots. Non-linear Eyring plot behaviour has been observed previously in the J–K epoxidation,[40] and has been interpreted in terms of the iso-inversion theory,[41] but the results have been contested.[42] In the current case, we have ignored the apparent non linearity, as it only appears close to the end of the temperature range, and the deviation may be statistically insignificant. The slope determined from the assumption of linearity will be qualitatively correct over most of the temperature range. We have been careful not to draw conclusions based on quantitative interpretation of the Eyring plots.

$$R\ln(\mathrm{er}) = R\ln\left(\frac{k_{\mathrm{major}}}{k_{\mathrm{minor}}}\right) = \frac{-\Delta\Delta H^{\neq}}{T} + \Delta\Delta S^{\neq} \qquad (1)$$

In the linear least-square plots in Fig. 9, the slopes and intercepts represent the differences in the activation enthalpy and entropy, respectively, for the formation of the major *vs* the minor enantiomer. The negative slopes mean that there is generally a strong enthalpic preference in the transition state for the formation of the minor enantiomer and the positive intercepts mean that the major enantiomer is favoured by entropy. The relative activation parameters ($-\Delta\Delta H^{\ddagger}$ and $\Delta\Delta S^{\ddagger}$) are given in the bottom rows of Tables 7 and 8. Modulation of the enantioselectivities of catalyst **2** may be expected mainly where the approach of a substrate is affected

by the presence of a receptor **3** molecule, as in states *c2* and *d2* (Fig. 5), or where the distribution of axial ligands on the catalytic Mn centre is affected, as in states *c1* and *d1*. Since the proportion of **2** in the corresponding states, *c* and *d*, is relatively constant over the temperature range (see χ_c and χ_d in Table 3 and Fig. 7), the temperature-dependent variation of the proportions of the different states of **2** has most likely only minor contribution to the observed trends in enantioselectivity. The direct effect of receptor **3** on the enantioselectivities of catalyst **2** is mainly of entropic origin (see Table 7). The entropic preference for the major enantiomer is reduced by the hydrogen-bonded attachment of the receptor to the catalytic site, reducing the conformational freedom of any substrate approaching the catalyst and probably destabilizing the transition state for the formation of the major enantiomer. An indirect enthalpic effect of receptor **3** arises from steric exclusion of certain axial ligands from the *endo* face of catalyst **2** in states *c* and *d*. In the case of receptor-binding substrate **7**, the formation of states *c* and *d* does not significantly affect the enthalpic parameter of enantioselectivity, but for the nonbinding substrate **6** the enthalpic preference for the minor enantiomer almost disappears upon formation of *c* and *d*. This can be seen from the slope for substrate **6** in Fig. 9 (compare ● and ○). Such a difference in enthalpy of activation suggests the involvement of different catalytic intermediates in the epoxidation of these two substrates.

In a series of epoxidations made in the same temperature range as the one above, using only nonbinding substrate **6**, the enthalpic parameter was completely turned around compared to the epoxidations using **6** and **7** in competition. It goes from -3.8 ± 1.9 kJ mol^{-1} (Table 7) in the presence of **7** to 2.6 ± 0.5 kJ mol^{-1} (Table 8) in the absence of **7**. It can thus be concluded that while the presence of receptor **3** results in a significant decrease in the enthalpic parameter and an increase in the entropic parameter, coordination of pyridine containing substances (substrate **7** or product **10**) to the catalytically active Mn species is the main contributor to the trend of increasing enantioselectivity with temperature. According to a study by Jacobsen *et al.*, on the electronic tuning of the enantioselectivity in J–K epoxidations by substitution in the 5 and 5′ positions on the salen ligand,[27] this is a rather extreme and unusual behaviour. However, there are examples of Mn(salen) catalysts that express similar temperature dependence on ee[43] and even of substrates with similar ee behaviour in standard J–K epoxidations.[44]

In the competitive epoxidations using system **2** + **3**, the difference in the enthalpy of activation for the two different enantiomers of the epoxide **9** from nonbinding substrate **6** lies approximately between the extremes for the presence and absence of substrate **7** (*vide supra*). This suggests that the catalytic species responsible for the epoxidation of **6** is to a lesser extent coordinated with pyridine-containing substances than the species transforming substrate **7**. This means that substrates **6** and **7** are predominantly epoxidised by two different catalytic species. These may be assigned to be the *exo* and *endo* faces of **2** in states *c* and *d* (Fig. 5). In this case, receptor-binding substrates (*i.e.* **7** and **8**) would be predominantly epoxidised by the *endo* face, having an unperturbed distribution of axial ligands L on the opposite *exo* face. In contrast, nonbinding substrates (*i.e.* **6**) would be predominantly epoxidised by the *exo* face, with steric perturbation of the distribution of L on the opposite *endo* face, since the later is occupied with a receptor-binding substrate or product.

Conclusion

The primary aim of this article has been to acquire understanding of what are the supramolecular structures responsible for the previously observed substrate selectivity in epoxidations using system **2** + **3**[4] and to find clues on how to improve the selectivity. We have used the modulation of several attributes of the catalytic performance of catalyst **2** by the presence of its complementary receptor unit **3**, with and without additional reaction components, to pull together an idea of the mechanism of its substrate selectivity.

First of all, the foundations necessary for the analysis of our system were clarified: the proportions of the different supramolecular states of catalyst **2**, including macrocycle **1**, and the nature of the catalytically active Mn species in the J–K epoxidation. The earlier assumption that macrocycle **1** was the predominant state of catalyst **2** in system **2** + **3** was refuted by careful solution analysis using a complete association model for the metal-free system **4** + **5**. The competitive coordination hypothesis was developed based on experimental results and recent literature observation on the J–K epoxidation. Based on these foundations, the catalytic behaviour of **2** and system **2** + **3** was analysed, and the effects of each reaction component were determined.

In the absence of other factors, the reactivity of **2** in the catalytic epoxidation of olefins is increased by the presence of donor ligands such as pyridine-containing substrate **7** and/or *N*-oxide **12**, as expected. The effect of receptor **3** appears to hinder the access of **12** to the Mn center in **2**, but on the other hand receptor **3** does not have any affect on the reactivity of **2** in the absence of **7**. The presence of **7** represses the reactivity of **2** by blocking the access of the *endo* face in state *c* and *d*, most probably because **3** retards the release and/or binding of the pyridine containing substrate **7** and/or its corresponding product **10**. Our results support the conclusion that receptor **3** is saturated with pyridine ligands **7** or **10**, meaning that mainly **7** can be epoxidised inside the supramolecular cavity at the expense of nonbinding substrates. It follows from this that in the absence of **7**, nonbinding substrate **6** can be epoxidised by both the *endo*- or *exo* face of **2**. The stability of **2** is greatly increased in the presence of **3**, but once again the presence of a pyridine entity destabilizes catalyst **2**. Plotting substrate selectivity as a function of conversion (Fig. 6b) revealed that at very low conversions, *N*-oxide **12** suppresses the substrate selectivity, while at higher conversions pyridine-containing epoxide **10** does so as well. This suggests that the epoxide oxygen of **10** gets a competitive advantage for coordination to Mn, since **10** is preorganized inside the cavity by coordination of its pyridine moiety to receptor **3**, resulting in signs of product inhibition.

Substrate selectivity was shown not to vary greatly within the temperature range from 233 to 313 K. This was explained by the small variations in the proportion of **2** in states contributing to substrate selectivity (states *c* and *d* in Fig. 5) within this temperature range. Substrate selectivity data at different concentrations of **2** and **3** at 298 K were used to demonstrate that macrocycle **1** (state *d*) was not the only substrate selective species in solution but also oligomers where **2** is hydrogen-bonded to at least one porphyrin receptor **3** (state *c*). The inherent selectivity of state *c* and *d* could however not be estimated since the mechanism of the J–K epoxidation is unclear. The major conclusion from the ee

investigations is that the orientation of the olefinic group of the receptor binding substrate **7** adopts an unfavourable orientation upon coordination to receptor **3** inside the cavity of states *c2* and *d2* resulting in a low ee of the product **10**. The higher spacer flexibility in receptor binding substrate **8** alleviates this orientational ee penalty, giving rise to higher ee in product **11**. It was also concluded that the presence of a pyridine ligand reverses the enthalpy contribution to enantioselectivity in the epoxidation.

The general picture of the supramolecular system **2** + **3** that emerges from these observations shows that the two states of catalyst **2** showing the greatest substrate selectivity, *c* and *d*, make up for 20 to 40% of total active catalyst in the epoxidation experiments, depending on reaction conditions. Formation of states *c* and *d* makes the *endo* face of the catalyst less accessible towards nonbinding substrates, oxidant and all other potential ligands, since there is always a pyridine-containing substance coordinating to receptor **3**, thus blocking the *endo* face of the catalyst **2**. Only substrates binding to the receptor (**7** and **8**) have easier access to the *endo* face than the *exo* face. Thus, states *c1* and *d1* are more exposed to the oxidant (PhIO) and substrates than *c2* and *d2* and are therefore more abundant and more reactive (Fig. 5). States *c1* and *d1* are completely nonselective towards substrates, while states *c2* and *d2* react more or less exclusively with receptor-binding substrates. The observed low substrate selectivity is thus due to the failure to suppress the formation of state *c1* and *d1*. Moreover, epoxide product **10** appears to be a slightly better guest for the cavity of states *c* and *d*, inducing signs of product inhibition in epoxidation. Compound **12** itself seems to inhibit substrate selectivity somewhat at low conversion, suggesting that it further limits the access of oxidant to the *endo* face and thus lowering the proportion of the substrate-selective states *c2* and *d2*, to the benefit of state *c1* and *d1*.

The competitive coordination hypothesis on the nature of the catalytic oxygen donating species in J–K epoxidations, proposed in this article, has been invaluable in the interpretation of experimental results. It is a viable, chemically sound alternative for explaining the dependence of the catalytic performance and selectivity of Mn(salen) epoxidation catalysts on the nature of the counterion, stoichiometric oxidant and added donor ligands.

In summary, we have designed and prepared a flexible, dynamic supramolecular catalytic system with the aim to achieve substrate selectivity, keeping rigidity at a minimum and system assembly and substrate binding rates at a maximum, in order to minimise the problems of catalytic cycle arrest and product inhibition, commonly observed in supramolecular catalysts. However binding or release of substrate **7** or product **10** seems to be the rate limiting step, and the system does show signs of product inhibition. The substrate selectivity is less than optimal, but we have now established the main reason for this, the unhindered reactivity of the *exo* face of catalyst **2** in states *c* and *d* as well of the presence of the non-selective states *a* and *b*. This, together with the complete solution analysis of metal-free system **4** + **5** is providing clues on how to improve the assembly of the catalyst as well as its substrate selectivity. A new and improved version of the current system is thus to be anticipated, that will further demonstrate the applicability of highly dynamic, kinetically labile supramolecular systems in substrate-selective catalysis. We are also currently working on developing a more elaborate studies of the kinetics- and enantioselectivities using Cr–salen, since substituting Mn for Cr makes it possible to study the kinetics starting from the stoichiometric Cr=O complex, which would remove many complicating factors. We would only be looking at the selectivity-determining step, not at the entire catalytic cycle.[31,45] The last point will help the present investigation to further clarify many aspects of system **2** + **3**, like clarifying the rate limiting step of the system **2** + **3**, the origin of the observed trends in enantioselectivity with temperature in the presence of **7**, as well as to quantify the selectivity of the different states.

Experimental

General

All commercial chemicals were used as received, unless otherwise noted. CH_2Cl_2 was distilled from CaH_2 and stored over molecular sieves. PhIO was prepared by hydrolysis of iodobenzene *I*,*I*-diacetate following a literature procedure.[46] TLC analyses (Merck 60 F_{254} sheets) were visualised under UV light (254 nm). Column chromatography was performed with silica gel (Matrex 0.063–0.200 mm). The diameter and height of columns are given in parenthesis as ($d \times h$ cm). Melting points were determined in capillary tubes, using a Sanyo GallenKamp melting point apparatus and are uncorrected. Infrared spectra were recorded on a Shimadzu FTIR-8300 spectrometer. NMR spectra of synthetic products were recorded on a Bruker DRX400 NMR spectrometer using $CDCl_3$ as solvent. NMR spectra for dilution experiments were recorded on a Varian Unity Inova 500 NMR spectrometer. Chemical shifts are given in ppm relative to TMS, using the residual solvent peaks at 7.27 (^{1}H) and 77.23 (^{13}C) as internal standards. Assignments were accomplished by coupling constants and integrals, as well as 2D correlation experiments when necessary. Elemental analyses were performed by A. Kolbe, Mikroanalytisches Laboratorium, Germany. Evaporation and concentration to dryness always refers to the use of a rotary evaporator under reduced pressure (*ca.* 10 mmHg). Filtration always refers to suction filtration on a glass frit type of filter, assisted with either a water pump or a membrane pump. *In vacuo* refers to pressures around 0.1–0.5 mmHg, obtained by the use of an oil pump.

GC chromatography was performed on a Perkin-Elmer Autosystem XL gas chromatograph. Column: Varian FactorFour capillary column, VR-1 ms, 30 m × 0.25 mm × 0.25 μm. Detector: FID. Chromatograms were analysed using Perkin-Elmer Turbochrom Navigator ver. 6.1.1.0.0:K20 software. For determination of ee GC chromatography was performed on a Perkin-Elmer Autosystem gas chromatograph. Column: Supelco Beta DEX 120(tm) capillary column, 30 m × 0.25 mm × 0.25 μm. Detector: FID. Carrier gas: Helium. Flow: 1 mL min^{-1}. The chromatograms were analyzed using Perkin-Elmer Turbochrom Navigator ver. 6.2.1.0.0:0104 software.

Synthesis

7-Bromo-4-hexyl-3-pentyl-1*H*-quinolin-2-one (23). Et_3N (50 mL, 350 mmol) was added dropwise under argon with mechanical stirring, to a solution of heptanoyl chloride (50 g, 340 mmol) in dry ether (200 mL) at a sufficient rate as to maintain a gentle reflux (*ca.* 20 min). Stirring was continued at rt for 2 h. The reaction flask was tightly closed and left standing overnight.

The formed precipitate was filtered off under a stream of argon and washed on the filter with dry ether (4 × 100 mL). The filtrate was concentrated to dryness, leaving 31.9 g (85%) of the ketene dimer **21** as a yellowish oil: δ_H (300 MHz, $CDCl_3$) 4.70 (1 H, t, J = 7.6 Hz), 3.94 (1 H, t, J = 7.1 Hz), 2.11 (2 H, m), 1.76 (2 H, m), 1.55–1.20 (12 H, m), 0.90 (6 H, m). This oil was dissolved in dry toluene (130 mL) and treated with freshly distilled 3-bromoaniline (23.2 g, 135 mmol). The solution was refluxed under argon overnight. After cooling to rt, it was washed with sat. $NaHCO_3$ (2 × 100 mL) and 1 M HCl (2 × 100 mL), dried ($MgSO_4$) and concentrated to give 54.0 g (100%) of ketoamide **22** as a brown oil that was pure enough to use in the next step: δ_H (300 MHz, $CDCl_3$) 8.55 (1 H, s), 7.82 (1 H, s), 7.42 (1 H, d, J = 7.9 Hz), 7.28–7.15 (2 H, m), 3.55 (1 H, t, J = 7.3 Hz), 2.60 (2 H, t, J = 7.3 Hz), 1.89 (2 H, m), 1.60 (2 H, m), 1.45–1.15 (12 H, m), 0.88 (6 H, m). The oil was dissolved in 96% H_2SO_4 (500 mL) and the solution was stirred at 80 °C for 2 h and then poured on ice (2 kg). The acid was neutralized by dropwise addition of concentrated NH_4OH (650 mL) with cooling on ice. The water phase was then extracted with $CHCl_3$ (3 × 750 mL). The combined organic phases were dried (Na_2SO_4) and concentrated, yielding a dark, sticky syrup. Two main products, **23** and an unidentified substance, in a ratio of 10 : 11 were detected by crude product NMR. Crystallisation from abs. EtOH gave 17.2 g (33%) of pure **23** as light beige crystals: mp 165–166 °C; R_f (heptane–EtOAc 1 : 1) 0.70; anal. calc. for $C_{20}H_{28}BrNO$: C, 63.49; H, 7.46; N, 3.70; found C, 63.36; H, 7.45; N, 3.74; IR (KBr) cm^{-1} 1655, 1558, 926; δ_H (400 MHz, $CDCl_3$) 10.96 (1 H, s), 7.52 (1 H, d, J = 8.7 Hz), 7.44 (1 H, d, J = 1.9 Hz), 7.31 (1 H, dd, J = 8.7 Hz, J = 1.9 Hz), 2.85 (2 H, m), 2.71 (2 H, m), 1.65–1.30 (14 H, m), 0.98–0.88 (6 H, m); δ_C (100 MHz, $CDCl_3$) 163.4, 147.1, 138.0, 131.9, 125.9, 125.4, 122.9, 119.1, 118.4, 32.2, 31.6, 29.9, 29.8, 29.0, 28.9, 27.0, 22.6, 22.5, 14.1 (2C); HRMS (FAB+) m/z calc. for $C_{20}H_{29}BrNO$ $[M + 1]^+$: 378.1433; found 378.1435.

4-Hexyl-2-oxo-3-pentyl-1,2-dihydroquinoline-7-boronic acid (13). At −78 °C, *n*-BuLi (2.5 M in hexanes, 36 mL, 90 mmol) was added dropwise during 20 min to a solution of quinolone **23** (11.35 g, 30.00 mmol) in anhydrous THF (250 mL). The solution turned dark orange-red and slightly turbid. It was stirred at −78 °C for 30 min before $B(OiPr)_3$ (20.9 mL, 90.0 mmol) was added dropwise during 10 min. The cooling bath was then removed, allowing the reaction mixture to reach rt. Upon warming, the color and turbidity disappeared. 1 M HCl (250 mL) was added and the mixture was stirred vigorously for 10 min before adding EtOAc (200 mL) and separating the phases. The aqueous phase was extracted with EtOAc (3 × 100 mL). The combined organic phases were washed with brine (200 mL), dried ($MgSO_4$) and concentrated to yield 16.13 g of a mixture of products as a sticky semisolid, which solidified upon trituration with MeOH. Repeated fractional crystallization from EtOAc afforded 3.99 g (39%) of quite pure boronic acid **13**. To obtain a sample suitable for characterisation, a small amount of **13** was refluxed with 2 equivalents of ethylene glycol in toluene, followed by recrystallization from MeCN to afford the analytically pure dioxaborolane derivative: mp 165–167 °C; anal. calc. for $C_{22}H_{32}BNO_3$: C, 71.55; H, 8.73; N, 3.79; found C, 71.46; H, 8.67; N, 3.83; IR (KBr) cm^{-1} 1651, 1408, 1385; δ_H (400 MHz, $CDCl_3$) 9.42 (1 H, s), 7.68 (1 H, d, J = 8.1 Hz), 7.61 (1 H, d, J = 8.2 Hz), 7.58 (1 H, s), 4.43 (4 H, s), 2.88 (2 H, m), 2.72 (2 H, m), 1.67–1.30 (14 H, m), 0.93 (6 H, t, J = 7.0 Hz); δ_C (100 MHz, $CDCl_3$) 162.6, 147.1 136.2, 133.0, 128.5 (br, w, *C*–B), 127.9, 123.9, 122.5, 122.0, 66.2, 32.2, 31.6, 29.9, 29.8, 29.0, 28.9, 27.2, 22.60, 22.58, 14.1 (2C); HRMS (FAB+) m/z calc. for $C_{22}H_{33}BNO_3$ $[M + 1]^+$: 370.2553; found 370.2560.

(1*S*,2*S*) - (−) - 1,2 - Bis(*tert* - butoxycarbonylamino) - 1,2 - bis(4-hydroxyphenyl)ethane (27). (1*S*,2*S*)-(−)-1,2-Bis(4-hydroxyphenyl)ethane-1,2-diammonium dibromide (**26**$(HBr)_2$, 5.07 g, 12.5 mmol), Boc-anhydride (7.15 g, 32.7 mmol) and $NaHCO_3$ (3.71 g, 44.1 mmol) were dissolved in THF–H_2O (1 : 1, 150 mL). The mixture was stirred at rt overnight. The phases were separated and the aqueous phase was extracted with ether (4 × 50 mL). The combined organic phases were washed with brine (100 mL), dried (Na_2SO_4) and concentrated to dryness. The residue was purified by chromatography (5 × 20 cm, eluent: heptane–EtOAc 1 : 1) to afford 3.43 g (62%) of **27** as a white powder: mp 211–212 °C; R_f (heptane–EtOAc 1 : 1) 0.20; $[\alpha]_D^{20}$ −8.6 ± 0.4° (*c* 0.822 in MeCN); anal. calc. for $C_{24}H_{32}N_2O_6$: C, 64.85; H, 7.26; N, 6.30; found C, 64.73; H, 7.18; N, 6.23; IR (KBr) cm^{-1} 3366, 2979, 1676, 1517, 1241, 1167; δ_H (400 MHz, DMSO-d_6) 9.15 (2 H, s), 7.16 (2 H, d, J = 6.9 Hz), 7.00 (4 H, d, J = 8.2 Hz), 6.59 (4 H, d, J = 8.0 Hz), 4.71 (2 H, d, J = 7.7 Hz), 1.28 (18 H, s); δ_C (100 MHz, DMSO-d_6) 155.8 (2C), 155.1 (2C), 131.5 (2C), 127.9 (4C), 114.5 (4C), 77.6 (2C), 58.4 (2C), 28.1 (6C); HRMS (FAB+) m/z calc. For $C_{24}H_{33}N_2O_6$ $[M + 1]^+$: 444.2260; found 444.2332.

The (1*R*,2*R*)-(+) enantiomer was prepared in the same manner: $[\alpha]_D^{20}$ +11.4 ± 0.5° (*c* 0.818 in MeCN).

(1*S*,2*S*)-(+)-1,2-Bis(*tert*-butoxycarbonylamino)-1,2-bis(4-decyloxyphenyl)ethane (28). K_2CO_3 (4.11 g, 29.7 mmol) was added to a solution of (*S*,*S*)-(−)-diphenol **27** (3.31 g, 7.43 mmol), decyl bromide (6.57 g, 29.7 mmol) and 18-crown-6 (78 mg, 0.30 mmol) in an anhydrous 1 : 1 DMF–THF mixture (200 mL). The reaction mixture was refluxed under argon and the progress of the reaction was monitored by TLC. After 48 h, the mixture was allowed to reach rt. Then water (200 mL) and ether (100 mL) were added and the phases were separated. The aqueous phase was extracted with ether (3 × 100 mL). The combined organic phases were washed with brine (100 mL), dried (Na_2SO_4) and concentrated to dryness. The residue was purified by chromatography (9 × 12 cm, eluent: heptane–EtOAc 4 : 1), followed by recrystallization from abs. EtOH to afford 3.44 g (64%) of **28** as a white solid: mp 137–138 °C (EtOH); R_f (heptane–EtOAc 4 : 1) 0.27; $[\alpha]_D^{20}$ +14.9 ± 0.6° (*c* 0.787 in $CHCl_3$); anal. calc. for $C_{44}H_{72}N_2O_6$: C, 72.89; H, 10.01; N, 3.86; found C, 73.08; H, 10.09; N, 3.94; IR (KBr) cm^{-1} 3375, 2923, 1680, 1513, 1245, 1177; δ_H (400 MHz, $CDCl_3$) 6.95 (4 H, d, J = 8.3 Hz), 6.71 (4 H, d, J = 8.6 Hz), 5.46 (2 H, br s), 4.79 (2 H, br s), 3.87 (4 H, t, J = 6.6 Hz), 1.73 (4 H, tt, J = 6.9 Hz, J = 6.6 Hz), 1.44 (18 H, s), 1.45–1.20 (28 H, m), 0.89 (6 H, t, J = 7.0 Hz); δ_C (100 MHz, $CDCl_3$) 158.7 (2C), 156.4 (2C), 131.7 (2C), 128.7 (4C), 114.6 (4C), 79.8 (2C), 68.2 (2C), 60.2 (2C), 32.1 (2C), 29.78 (2C), 29.77 (2C), 29.6 (2C), 29.53 (2C), 29.50 (2C), 28.6 (6C), 26.3 (2C), 22.9 (2C), 14.3 (2C); HRMS (FAB+) m/z calc. For $C_{44}H_{71}N_2O_6$ $[M - 1]^+$: 723.5312; found 723.5321.

The (1*R*,2*R*)-(−) enantiomer was prepared in the same manner: $[\alpha]_D^{20}$ −9.5 ± 1.1° (*c* 0.764 in $CHCl_3$).

(1*S*,2*S*)-(−)-1,2-Bis(4-decyloxyphenyl)ethane-1,2-diammonium bis(trifluoroacetate) (15·(TFA)$_2$). TFA (30 mL) was added to a solution of Boc-protected diamine **28** (2.25 g, 3.10 mmol) in CH_2Cl_2 (30 mL). The solution was stirred at rt under argon for 1 h. Evaporation of volatiles with repeated azeotropic evaporation with CH_2Cl_2 and toluene afforded 2.33 g (100%) of pure **15**(TFA)$_2$ as a light beige solid: mp 141–142 °C; R_f (heptane–EtOAc 1 : 1) 0.46; $[\alpha]_D^{20}$ −79.7 ± 0.7° (*c* 0.922 in $CHCl_3$); anal. calc. for $C_{38}H_{58}F_6N_2O_6$: C, 60.62; H, 7.77; N, 3.72; found C, 60.71; H, 7.68; N, 3.80; IR (KBr) cm^{-1} 3100–2980 (br), 2920, 2851, 1680, 1613, 1517, 1248, 1210, 1141; δ_H (400 MHz, $CDCl_3$) 7.01 (4 H, d, J = 8.6 Hz), 6.74 (4 H, d, J = 8.6 Hz), 4.74 (2 H, s), 3.86 (4 H, t, J = 6.6 Hz), 1.73 (4 H, tt, J = 6.9 Hz, J = 6.6 Hz), 1.45–1.20 (28 H, m), 0.89 (6 H, m); δ_C (100 MHz, $CDCl_3$) 160.4 (2C), 129.0 (4C), 124.9 (2C), 115.5 (4C), 68.4 (2C), 58.7 (2C), 32.1 (2C), 31.8 (2C), 29.8 (2C), 29.6 (2C), 29.5 (2C), 29.4 (2C), 26.2 (2C), 22.9 (2C), 14.3 (2C); HRMS (FAB+) *m*/*z* calc. For $C_{34}H_{54}NO_2$ [M-2(TFA$^-$)− NH_4^+]$^+$: 508.4149; found 508.4154.

The (1*R*,2*R*)-(+) enantiomer was prepared in the same manner: $[\alpha]_D^{20}$ +75.7 ± 0.5° (*c* 0.921 in $CHCl_3$).

3-*tert*-Butyl-5-(4-hexyl-2-oxo-3-pentyl-1,2-dihydroquinolin-7-yl)-2-hydroxybenzaldehyde (24). A two phase mixture of boronic acid **13** (3.60 g, 10.5 mmol), iodosalicylaldehyde **14** (2.89 g, 9.50 mmol), 2 M Na_2CO_3 (7.9 mL, 15.8 mmol), EtOH (4.4 mL) and toluene (80 mL) was degassed by argon bubbling for 15 min. $Pd(PPh_3)_4$ (0.30 g, 0.26 mmol) was added and the mixture was refluxed with efficient stirring for 3 h. Upon cooling, the product precipitated. It was collected by filtration and washed on the filter with water, EtOH and toluene. The filtrate was extracted with EtOAc (2 × 75 mL). The extract was dried (Na_2SO_4) and evaporated, yielding additional crude product. The two fractions were combined and eluted through a pad of silica (6 × 5 cm, eluent: $CHCl_3$–EtOH 99 : 1), followed by recrystallization from abs. EtOH (350 mL), to afford 2.70 g (60%) of **24** as small shiny off-white plates: mp 187–188 °C; R_f (heptane–EtOAc 1 : 1) 0.56; anal. calc. for $C_{31}H_{41}NO_3$: C, 78.28; H, 8.69; N, 2.94; found C, 78.19; H, 8.70; N, 3.01; IR (KBr) cm^{-1} 3444 (br), 1635 (br), 1551; δ_H (400 MHz, $CDCl_3$) 11.87 (1 H, s), 11.32 (1 H, br s), 10.01 (1 H, s), 7.85 (1 H, d, J = 2.2 Hz), 7.75 (1 H, d, J = 8.5 Hz), 7.71 (1 H, d, J = 2.2 Hz), 7.48 (1 H, d, J = 1.7 Hz), 7.42 (1 H, dd, J = 8.5, J = 1.7 Hz), 2.91 (2 H, m), 2.76 (2 H, m), 1.70–1.29 (14 H, m), 1.51 (9 H, s), 0.94 (3 H, t, J = 7.0 Hz), 0.88 (3 H, t, J = 7.2 Hz); δ_C (100 MHz, $CDCl_3$) 197.2, 163.8, 161.1, 147.3, 140,7, 139.0, 137.6, 133.0, 131.3, 131.2, 130.2, 125.1, 120.9, 120.8, 119.3, 113.4, 35.1, 32.3, 31.6, 30.0, 29.9, 29.2 (3C), 29.1, 29.0, 27.0, 22.62, 22.58, 14.1, 14.0; HRMS (FAB+) *m*/*z* calc. For $C_{31}H_{42}NO_3$ [M + 1]$^+$: 476.3165; found 476.3163.

***N*,*N*′-Bis(3-*tert*-butyl-5-[4-hexyl-2-oxo-3-pentyl-1,2-dihydroquinolin-7-yl]salicylidene)-(1*R*,2*R*)-1,2-bis(4-decyloxy-phenyl)-ethane-1,2-diamine (4).** The ammonium salt **15**(TFA)$_2$ (*ca.* 0.6 g) was dissolved in CH_2Cl_2 and neutralized by dropwise addition of 1 M NaOH (10 mL). The aqueous phase was extracted with CH_2Cl_2, dried (Na_2SO_4) and concentrated to afford the free diamine **15** (419 mg, 0.79 mmol) as a shiny white powder. It was dissolved in toluene (15 mL) and then salicylaldehyde **24** (751 mg, 1.58 mmol) and EtOH (30 mL) were added. The mixture was refluxed under argon for 10 h. After cooling, the solvents were evaporated and the residue was purified by chromatography (5 × 14 cm, eluent: heptane–EtOAc 4 : 1), affording 803 mg (70%) of **4** as a bright yellow solid: mp 115–116 °C; R_f (heptane–EtOAc 1 : 1) 0.65; $[\alpha]_D^{20}$ +61.8 ± 0.4° (*c* 0.542 in $CHCl_3$); anal. calc. for $C_{96}H_{134}N_4O_6$: C, 80.06; H, 9.38; N, 3.89; found C, 79.96; H, 9.35; N, 3.93; IR (KBr) cm^{-1} 3390, 2925, 2854, 1653, 1618, 1511, 1247, 1171; δ_H (400 MHz, $CDCl_3$) 14.04 (2 H, s), 10.47 (2 H, s), 8.44 (2 H, s), 7.66 (2 H, d, J = 8.6 Hz), 7.55 (2 H, s), 7.32–7.24 (6 H, m), 7.15 (4 H, d, J = 8.7 Hz), 6.80 (4 H, d, J = 8.7 Hz), 4.73 (2 H, s), 3.91 (4 H, t, J = 6.6 Hz), 2.87 (4 H, m), 2.70 (4 H, m), 1.76 (4 H, tt, J = 7.4 Hz, J = 6.6 Hz), 1.65–1.20 (56 H, m), 1.45 (18 H, s), 0.96–0.82 (18 H, m); δ_C (100 MHz, $CDCl_3$) 166.4 (2C), 163.4 (2C), 160.4 (2C), 158.5 (2C), 147.2 (2C), 141.6 (2C), 137.9 (2C), 137.4 (2C), 131.2 (2C), 130.9 (2C), 129.5 (2C), 129.0 (4C), 128.5 (2C), 128.4 (2C), 128.2 (2C), 125.3 (2C), 124.8 (2C), 120.9 (2C), 118.8 (2C), 114.4 (4C), 112.8 (2C), 79.5 (2C), 68.0 (2C), 35.0 (2C), 32.2 (2C), 31.9 (2C), 31.6 (2C), 30.0 (2C), 29.9 (2C), 29.6 (2C), 29.5 (2C), 29.4 (6C), 29.3 (2C), 29.2 (2C), 29.1 (2C), 28.9 (2C), 27.0 (2C), 26.0 (2C), 25.7 (2C), 22.67 (2C), 22.62 (2C), 22.57 (2C), 14.11 (2C), 14.08 (2C), 14.03 (2C); HRMS (FAB+) *m*/*z* calc. For $C_{96}H_{135}N_4O_6$ [M + 1]$^+$: 1440.0382; found 1440.0381.

[*N*,*N*′-Bis(3-*tert*-butyl-5-[4-hexyl-2-oxo-3-pentyl-1,2-dihydroquinolin-7-yl]salicylidene)-(1*R*,2*R*)-1,2-bis(4-decyloxy-phenyl)-ethane-1,2-diamine]manganese(III) chloride (2). $Mn(OAc)_2·4H_2O$ (382 mg, 1.56 mmol) was added to a yellow suspension of salen ligand **4** (748 mg, 0.52 mmol) in abs. EtOH (25 mL) and $CHCl_3$ (10 mL). The mixture immediately took a brown colour. It was refluxed in air for 1 h, and during the last 30 min, air was bubbled through the refluxing mixture. Then, LiCl (110 mg, 2.60 mmol) was added and the dark brown mixture was refluxed for 1 h. After cooling to rt, the mixture was concentrated to approx. half the original volume, removing most of the $CHCl_3$ to induce precipitation. The product was collected by filtration and washed with water (3 × 10 mL) and ether (2 × 10 mL). After air drying on the filter, the solid was dissolved in $CHCl_3$–MeOH 19 : 1. Evaporation of the solvent and drying *in vacuo* at 40 °C overnight afforded 746 mg (94%) of **2** as a brown solid: mp 213–214 °C; R_f ($CHCl_3$–MeOH 19 : 1) 0.21; $[\alpha]_D^{20}$ 2990° (*c* 0.157 in $CHCl_3$); anal. calc. for $C_{96}H_{132}ClMnN_4O_6$: C, 75.44; H, 8.70; N, 3.67; found C, 75.51; H, 8.78; N, 3.72; IR (KBr) cm^{-1} 1647, 1602; HRMS (FAB+) *m*/*z* calc. for $C_{96}H_{132}MnN_4O_6$ [M − Cl]$^+$: 1491.9527; found 1491.9535.

3-Decyloxy-5-hydroxymethylphenol (30). K_2CO_3 (2.07 g, 15.0 mmol), 18-crown-6 (79 mg, 0.3 mmol) and bromodecane (3.32 g, 15.0 mmol) were successively added to a solution of phenol **29** (6.31 g, 45.0 mmol) in acetone (125 mL). The reaction mixture was refluxed under a $CaCl_2$ drying tube for 27 h. The solvent was evaporated and the remaining brown tar was triturated first with $CHCl_3$ (3 × 100 mL) and then with acetone (3 × 100 mL). Unreacted **29** (3.4 g) was recovered by evaporation of the acetone washings. The $CHCl_3$ was evaporated and the crude product was purified by a pad of silica (4.5 × 10 cm). The side product eluted through the pad with $CHCl_3$ and **30** with $CHCl_3$–methanol 97 : 3, affording 2.76 g (66% from bromodecane) of pure **30** as a white powder: mp 66.2 °C; anal. calc. for $C_{17}H_{28}O_3$: C, 72.82; H, 10.06; found C, 72.74; H, 9.98; IR (KBr) cm^{-1} 3378.3, 3064.7, 2916.2, 1600.8; δ_H (400 MHz, $CDCl_3$) 6.49 (1 H, m), 6.44 (1 H, m), 6.33 (1 H, m), 5.19 (1 H, s), 4.61 (2H, s), 3.93 (2 H, t, J = 6.6 Hz), 1.80–1.73 (3 H, m), 1.46–1.23 (14 H, m), 0.91–0.87 (3 H, m); δ_C

(100 MHz, $CDCl_3$) 160.70, 156.92, 143.42, 105.94, 105.41, 101.17, 68.12, 65.19, 31.88, 29.57, 29.55, 29.37, 29.31, 29.20, 26.02, 22.67, 14.11. HRMS (EI^+): m/z calc. for $C_{17}H_{28}O_3$, $[M]^+$: 280.2038; found 280.2056.

3-(*tert*-Butyldimethylsilanyloxymethyl)-5-decyloxyphenol (31). Alcohol **30** (11.7 g, 41.8 mmol), imidazole (8.50 g, 124 mmol) and TBDMSCl (6.30 g, 41.8 mmol) were dissolved in DMF (210 mL) and the mixture was stirred at rt for 24 h. Water was added and the resulting mixture was extracted with ether (4 × 100 mL). The combined organic phases were washed with brine (2 × 100 mL) and dried (Na_2SO_4). The solvent was evaporated to afford 16.5 g (99%) of **31** as a clear oil: R_f (heptane–EtOAc 4 : 1) 0.44; anal. calc. for $C_{23}H_{41}O_3Si$: C, 70.00; H, 10.73; found C, 69.81; H, 10.64; δ_H (400 MHz, $CDCl_3$) 6.46 (1 H, m), 6.40 (1 H, m), 6.28 (1 H, m) 5.03 (1 H, s), 4.66 (2 H, s), 3.92 (2 H, t, $J = 6.61$ Hz), 1.80–1.73 (2H, m), 1.44–1.28 (14 H, m), 0.95 (9 H, m), 0.90 (3 H, m), 0.12–0.10 (6 H, m). δ_C (100 MHz, $CDCl_3$) 160.39, 156.58, 144.18, 105.13, 104.52, 100.51, 68.04, 64.72, 31.88, 29.57, 29.55, 29.38, 29.31, 29.20, 26.02, 25.95, 22.67, 18.42, 14.10, −5.28; HRMS (EI+) m/z calc. for $C_{23}H_{42}O_3Si$ $[M + 1]^+$: 393.2825; found 393.2825.

Trifluoromethanesulfonic acid 3-(*tert*-butyldimethylsilanyloxymethyl)-5-decyloxyphenyl ester (20). Trifluoromethanesulfonic anhydride (1.17 mL, 7.00 mmol) was added as fast as possible to a solution of phenol **31** (2.75 g, 7.00 mmol) in pyridine (5 mL) at 0 °C under argon. White smoke formed during the addition. The reaction was stirred at 0 °C for 5 min, then for additional 17 h at rt. Water (50 mL) was added and the aqueous phase was extracted with ether (3 × 50 mL). The combined organic phases were washed with water, 10% HCl solution, water and brine, then dried ($MgSO_4$) and evaporated. The crude product (2.905 g) was purified by a pad of silica (2.5 × 5 cm, eluent: ether) to afford 2.78 g (75%) of **20** as a yellow oil: R_f (heptane–EtOAc 9 : 1) 0.83; anal. calc. for $C_{24}H_{41}F_3O_5SSi$: C, 54.73; H, 7.85; found C, 54.86; H, 8.03; δ_H (400 MHz, $CDCl_3$) 6.87 (1 H, m), 6.83 (1 H, m), 6.66 (1 H, m), 4.72 (2 H, s), 3.94 (2 H, t, $J = 6.55$ Hz), 1.82–1.75 (2 H, m), 1.45–1.29 (16 H, m), 1.00–0.95 (3 H, m), 0.88 (3 H, m), 0.10 (6 H, m). δ_C (100 MHz, $CDCl_3$) 160.21, 150.19, 145.26, 111.59, 110.31, 106.24, 68.57, 64.01, 31.88, 29.59, 29.53, 29.33, 29.30, 29.02, 25.95, 25.83, 22.67, 18.32, 14.10, −5.37. HRMS (EI+) m/z calc. for $C_{24}H_{41}F_3O_5SSi$ $[M - 1]^+$: 525.2318; found 525.2310.

2-Benzyloxy-4-iodopyridine (35). KOH (8.08 g, 145 mmol), 18-crown-6 (0.72 g, 2.70 mmol) and benzyl alcohol (7.53 mL, 72.4 mmol) were added to a solution of fluoropyridine **34**[17] (16.1 g g, 72.0 mmol) in toluene (600 mL). The reaction flask was fitted with a soxlet containing CaH_2 and sand. The mixture was refluxed for 3.5 h. After cooling to rt, water (200 mL) was added and the aqueous phase was extracted with toluene (2 × 200 mL). The combined organic phases were washed with a saturated KCl solution (300 mL) and dried ($MgSO_4$). The crude product (22.0 g) was purified by flash chromatography (11 × 20 cm, eluent: heptane–EtOAc 9 : 1) to afford 20.8 g (92%) of **35** as yellow oil: R_f (heptane–EtOAc 9 : 1) 0.32; anal. calc. for $C_{12}H_{10}INO$: C, 46.33; H, 3.24; N, 4.50, found C, 46.43; H, 3.31; N, 4.60; IR (neat film) cm^{-1} 3031.9, 2947.0, 2885.3; δ_H (400 MHz, $CDCl_3$) 7.86 (2 H, d, $J =$ 5.36 Hz), 7.5–7.31 (5 H, m), 7.27 (1 H, d, $J = 1.4$ Hz), 7.25 (1 H, dd, $J_1 = 5.36$ Hz, $J_2 = 1.4$ Hz), 5.39 (2 H, s); δ_C (100 MHz, $CDCl_3$) 163.80 (1C), 147.20 (1C), 137.02 (1C), 128.67 (2C), 128.14 (3C), 126.21 (1C), 120.86 (1C), 106.59 (1C), 68.07 (1C). HRMS (EI+) m/z cacl. for $C_{12}H_{10}INO$ $[M]^+$: 310.9807, found 310.9810.

2-(Benzyloxy)-4-(tributylstannanyl)pyridine (19). *n*-BuLi (2.5 M in hexane, 27.1 mL, 67.6 mmol) was added dropwise to a solution of **35** (19.1 g, 61.5 mmol) in dry ether (410 mL) at −78 °C. The solution was stirred for 4 h at the same temperature. Freshly distilled *n*-Bu_3SnCl (18.7 mL, 67.6 mmol) was added and the mixture was allowed to reach rt before water (200 mL) was added. The phases were separated and the aqueous phase was extracted with ether (2 × 100 mL). The combined organic phases were washed successively with water and brine, dried ($MgSO_4$) and the solvent was evaporated. The resulting oil was purified by chromatography (10.5 × 12 cm, eluent: heptane–EtOAc 49 : 1) to afford 28.2 g (96%) of **19** as a clear yellow oil: R_f (heptane–EtOAc: 49 : 1) 0.18; anal. calc. for $C_{24}H_{37}NOSn$: C, 60.78; H, 7.86; N, 2.95; found C, 60.65; H, 7.81; N, 2.90; δ_H (400 MHz, $CDCl_3$) 8.07 (1 H, d, $J = 4.8$ Hz), 7.54–7.46 (2 H, m), 7.45–7.29 (3 H, m), 6.98 (1 H, d, $J = 4.8$ Hz), 5.38 (2 H, s), 1.68–1.40 (6 H, m), 1.40–1.25 (6 H, m), 1.20–0.97 (6 H, m), 0.90 (9 H, t, $J = 7.43$ Hz); δ_C (100 MHz, $CDCl_3$) 162.5, 144.9, 137.4, 128.4, 128.0, 127.8, 124.6, 119.2, 67.5, 28.9, 27.3, 13.6, 9.6; HRMS (FAB+) m/z calc. for $C_{24}H_{37}NOSn$ $[M]^+$: 476.1975; found 476.1995.

2-(Benzyloxy)-4-[3-decyloxy-5-(*tert*-butyldimethylsilanyloxymethyl)phenyl]pyridine (36). A solution of organotin compound **19** (17.3 g, 36.4 mmol), triflate **20** (19.2 g, 36.4 mmol) and dried LiCl (4.62 g, 109 mmol) in freshly distilled DMF (182 mL) was degassed by argon bubbling for 5 min. $Pd(PPh_3)_4$ (1.26 g, 1.10 mmol) was added and the mixture was heated at 90 °C for 48 h. After cooling to rt, water (100 mL) was added and the mixture was extracted with heptane (3 × 200 mL). The solvent was evaporated and the crude product was eluted through a pad of silica using heptane–EtOAc (9 : 1) as the eluent. The solvent was evaporated and the residue was subjected to bulb-to-bulb distillation (0.4 mmHg, 100 °C, 4 h) to remove tin residues. The remaining oil was further purified by chromatography (12 × 15 cm, eluent: heptane–EtOac 95 : 5) to afford 9.6 g (47%) of **36** as clear yellow oil: R_f (heptane–EtOAc 4 : 1) 0.44; anal. calc. for $C_{35}H_{51}NO_3Si$: C, 74.82; H, 9.15; N, 2.49; found C, 74.73; H, 9.21; N, 2.55; IR (neat film) cm^{-1} 3031.9, 2927.7, 2854.5, 1604.7; δ_H (400 MHz, $CDCl_3$) 8.22 (1 H, d, $J = 5.4$ Hz), 7.52–7.30 (5 H, m), 7.15 (1 H, s), 7.13 (1 H, dd, $J = 1.24$ Hz, $J = 5.4$ Hz), 7.05–7.02 (2 H, m), 6.97 (1 H, s), 5.44 (2 H, s), 4.78 (2 H, s), 4.01 (2 H, t, $J = 6.56$ Hz), 1.84–1.78 (2 H, m), 1.51–1.24 (14 H, m), 0.97 (9 H, s), 0.90–0.87 (3 H, m), 0.13 (6 H, s); δ_C (100 MHz, $CDCl_3$) 164.30, 159.73, 151.45, 147.05, 143.83, 139.38, 137.35, 128.47, 127.95, 127.82, 116.75, 115.67, 112.64, 111.83, 108.84, 68.15, 67.75, 64.75, 31.88, 29.57, 29.55, 29.38, 29.31, 29.25, 26.03, 25.95, 22.67, 18.43, 14.11, −5.22; HRMS (FAB^+): m/z calc. for $C_{35}H_{51}NO_3Si$, $[M + 1]^+$ 562.3717; found 562.3714.

3-Decyloxy-5-(2-benzyloxypyrid-4-yl)benzaldehyde (16). DDQ (4.25 g, 18.7 mmol) was added in one portion to a solution of **36** (9.56 g, 17.0 mmol) in CH_2Cl_2 (500 mL). The resulting orange mixture was stirred at rt for 24 h. During the progress of the reaction a white solid precipitated. The mixture was filtered through a pad of neutral alumina, rinsing with ether. The solvent was evaporated and the crude product was purified by flash chromatography (6 × 18 cm, eluent: heptane–EtOAc 9 : 1) to

afford 6.50 g (85%) of **16** as a sticky clear yellow oil: R_f (heptane–EtOAc 4 : 1) 0.33; anal. calc. for $C_{29}H_{35}NO_3$: C, 78.17; H, 7.92; N, 3.14; found C, 78.29; H, 8.07; N, 3.22; IR (neat film) cm^{-1} 3031.9, 2923.9, 2854.5, 1701.1, 1604.7; δ_H (400 MHz, $CDCl_3$) 10.03 (1 H, s), 8.26 (1 H, d, $J = 5.36$ Hz), 7.69 (1 H, t, $J = 1.29$ Hz), 7.52–7.30 (7 H, m), 7.15 (1 H, dd, $J = 1.5$ Hz, $J = 5.36$ Hz), 7.06, (1 H, s), 5.45 (2 H, s), 4.07 (2 H, t, $J = 6.52$ Hz), 1.88–1.75 (2 H, m), 1.55–1.24 (14 H, m), 0.90–0.87 (3 H, m). δ_C (100 MHz, $CDCl_3$) 191.88, 164.61, 160.44, 149.93, 147.69, 140.65, 138.53, 137.40, 128.68, 128.07, 121.71, 120.27, 115.54, 113.58, 109.13, 68.80, 68.03, 32.08, 29.75, 29.74, 29.53, 29.51, 29.30, 26.18, 22.87, 14.31; HRMS (FAB^+): m/z cacl. for $C_{29}H_{35}NO_3$ $[M + 1]^+$: 446.2695; found 446.2689.

5-Decyloxy-2-iodo-1,3-dimethylbenzene (38). K_2CO_3 (64.0 g, 463 mmol) and bromodecane (42.0 mL, 200 mmol) were added to a solution of phenol **37**[19] (83.2 g, 154 mmol) in DMF (1.5 L) and the mixture was heated at 80 °C for 11 h. DMF was distilled off under reduced pressure (10 mmHg) and water was added to the residue and was extracted with $CHCl_3$ (3 × 200 mL). The combined organic phases were dried over $MgSO_4$ and the solvent was evaporated. The crude oil was purified by bulb-to-bulb distillation (0.4 mmHg, 85 °C), to afford 59.8 g (quantitative) of **38** as yellow oil: Anal calc. for $C_{18}H_{29}IO$: C, 55.67; H, 7.53; found C, 55.79; H, 7.56; IR (neat film) cm^{-1} 29.239.9, 2852.5, 1579.6; δ_H (400 MHz, $CDCl_3$) 6.68 (2 H, s), 3.92 (2 H, t, $J = 6.6$ Hz), 2.45 (6 H, s), 1.83–1.69 (2 H, m), 1.51–1.21 (14 H, m), 0.95–0.84 (3 H, m). δ_C (100 MHz, $CDCl_3$) 158.71, 142.72, 113.47, 96.71, 67.98, 31.89, 29.69, 29.56, 29.55, 29.36, 29.31, 29.22, 26.00, 22.68, 14.11. HRMS (FAB+) m/z calc. for $C_{18}H_{29}IO$ $[M]^+$ 388.1263; found 388.1266.

4-Decyloxy-2,6-dimethylbenzaldehyde (18). Compound **38** (15.8 g, 40.7 mmol), dried overnight at 0.4 mmHg, was dissolved in anhydrous diethylether (300 mL). *n*-BuLi (2.5 M in hexane, 19.5 mL, 48.8 mmol) was added dropwise at −78 °C. The reaction mixture was stirred at this temperature for 1.5 h before freshly distilled DMF (4.27 mL, 55.3 mmol) was added. The solution was allowed to reach 0 °C and then poured into a beaker with ice and was acidified to pH 1 with 37% HCl. The phases were separated and the aqueous phase was extracted with $CHCl_3$. The combined organic phases were washed with brine, dried ($MgSO_4$) and evaporated under reduced pressure. The crude product was collected as a yellow oil. It was purified by chromatography (12 × 9 cm, eluent: heptane–EtOAc 4 : 1) to afford 10.1 g, (85%) of **18** as a clear yellow oil: Anal. calc. for $C_{19}H_{30}O_2$: C, 78.57; H, 10.41; found C, 78.66; H, 10.36; IR (neat film) cm^{-1} 2924.8, 2854.5, 2359.7, 2340.5, 1679.9; δ_H (400 MHz, $CDCl_3$) 10.47 (1 H, s), 6.58 (2 H, s), 4.00 (2 H, t, $J = 6.6$ Hz), 1.82–1.75 (2 H, m), 1.51–1.2 (14 H, m), 0.91–0.87 (3 H, m). δ_C (100 MHz, $CDCl_3$) 191.5, 162.36, 144.41, 125.72, 115.29, 67.96, 31.86, 29.52 (2C), 29,30, 29.29, 29.07, 25.93, 22.65, 21.07, 14.08; HRMS (FAB+) m/z calc. for $C_{19}H_{30}O_2$ $[M]^+$: 290.2246; found 290.2250.

5-(4-Decyloxy-2,6-dimethylphenyl)dipyrromethane (17). A mixture of aldehyde **18** (16.4 g, 56.5 mmol) and freshly distilled pyrrole (98 mL, 25 equiv.) was degassed by argon bubbling under stirring until **18** was completely dissolved (approx. 10 min). TFA (5.65 mmol, 435 μL) was then added in one portion. The reaction mixture turned purple and then brown immediately after addition of the acid. It was stirred at rt for 1 h before quenching by addition of triethylamine (2 mL) and toluene (40 mL). The mixture was washed with brine (50 mL), dried (Na_2SO_4) and the solvents were evaporated (first on the evaporator at 10 mmHg keeping the temperature below 40 °C and then at 0.4 mmHg at rt). The resulting black oil was dissolved in CH_2Cl_2 and filtered through a pad of alumina (7 × 4 cm). The solvent was evaporated and the crude product was purified by bulb-to-bulb distillation (160–225 °C; 0.4–0.2 mmHg). The collected oil crystallised overnight in the fridge. It was further recrystallised from ethanol to afford 3.67 g (16%) of **17** as green crystals: mp 68.2–69.6 °C; anal. calc. for $C_{27}H_{38}N_2O$: C, 79.76, H, 9.42, N, 6.89; found C 79.88, H 9.34, N 6.81. IR (KBr) cm^{-1} 3379.1, 2850.6, 1596.9; δ_H (400 MHz, $CDCl_3$) 7.95 (2 H, bs), 6.74–6.65 (2 H, m), 6.61 (2 H, s), 6.24–6.15 (2 H, m), 6.07–5.95 (2 H, m), 5.90 (1 H, s), 3.95 (2 H, t, $J = 6.52$ Hz), 2.08 (6 H, s), 1.87–1.70 (2 H, m), 1.52–1.16 (14 H, m), 1.01–0.75 (3 H, m); δ_C (100 MHz, $CDCl_3$) 139.11, 131.43, 129.58, 116.06, 115.22, 108.60, 106.37, 67.72, 37.96, 31.88, 29.58, 29.55, 29.39, 29.31, 26.08, 22.67, 20.90, 12.11; HRMS (FAB^+): m/z calc. for $C_{27}H_{38}N_2O$ $[M]^+$ 406.2984; found 406.2973.

5,15-Bis[3-(2-benzyloxypyrid-4-yl)-5-decyloxyphenyl]-10,20-bis(4-decyloxy-2,6-dimethylphenyl)porphyrin (39). TFA (0.928 mL, 12.5 mmol) was added in one portion to a solution of aldehyde **16** (3.13 g, 7.02 mmol) and dipyrromethane **17** (2.86 g, 7.02 mmol) in CH_2Cl_2 (702 mL). The reaction mixture was stirred at rt for 3 h. DDQ (1.59 g, 7.02 mmol) was then added in one portion. The dark brown solution turned green and was stirred at rt for 1 h before filtering though a pad of dry neutral alumina (6 × 10 cm) eluting with CH_2Cl_2 (800 mL) until the eluent was clear green. The solvent was evaporated and the residue (2.903 g) was dissolved in toluene (140 mL) with an additional amount of DDQ (1.59 g, 7.02 mmol). The purple orange solution was refluxed for 1 h and after cooling to room temperature, it was filtered through a pad of dry neutral alumina (6 × 10 cm) and eluting with CH_2Cl_2 (750 mL) until the eluent was almost colourless. The solvent was evaporated to afford 1.39 g (23%) of **39** as a purple solid: Anal. calc. for $C_{112}H_{136}N_6O_6$, C, 80.92; H, 8.25; N, 5.06; found C, 80.98; H, 8.21; N, 4.95; IR (KBr) cm^{-1} 2922.0, 2852.5, 1598.9, 1548.7; δ_H (400 MHz, $CDCl_3$) 8.94 (4 H, d, $J = 4.5$ Hz) 8.79 (4 H, d, $J = 4.5$ Hz), 8.31 (2 H, d, $J = 5.4$ Hz), 8.14 (2 H, s), 7.91 (2 H, s), 7.63 (2 H, s), 7.57–7.48 (4 H, m) 7.44–7.29 (10 H, m), 7.08 (4 H, s), 5.48 (4 H, s), 4.35–4.20 (8 H, m), 2.08–1.85 (20 H, m), 1.74–1.20 (56 H, m), 1.02–0.85 (12 H, m), −2.57 (2 H, bs). δ_C (100 MHz, $CDCl_3$) 164.45, 158.99, 158.04, 141.14, 147.33, 143.98, 140.86, 140.79, 140.71, 137.59, 137.28, 133.62, 131.33, 130.38, 128.46, 127.98, 127.82, 125.94, 121.55, 118.55, 118.32, 115.91, 112.83, 112.66, 109.26, 68.54, 68.06, 67.80, 31.96, 31.87, 29.69–29.30 (10C), 26.28, 26.12, 22.73, 22.65, 22.05, 14.16, 14.10. UV λ_{max} (ether)/nm 418 (ε/dm^3 mol^{-1} cm^{-1} 41434), 513 (26521), 546 (21565), 591 ($\varepsilon = 20695$), 648 ($\varepsilon = 19391$); HRMS (FAB+) m/z calc. for $C_{112}H_{136}N_6O_6$ $[M]^+$: 1661.0521; found 1661.0464.

5,15-Bis(3-decyloxy-5-[2-oxopyrid-4-yl]phenyl)-10,20-bis(4-decyloxy-2,6-dimethylphenyl)porphyrin (5). Thioanisole (0.79 mL, 6.7 mmol) was added in one portion to a green solution of porphyrin **39** (1.39 g, 0.836 mmol) in the minimum amount of TFA required to dissolve all of **39**. The reaction mixture was stirred at rt for 24 h. TFA was evaporated to give a green residue. It was dissolved in ether and triethylamine was added dropwise until the solution became purple. The solvent was evaporated and the purple solid was triturated successively

with methanol, water and methanol and then dried *in vacuo* to afford 1.25 g (quantitative) of **5** as purple solid. Anal. calc. for $C_{98}H_{124}N_6O_6$: C, 79.42; H, 8.43; N, 5.67; found C, 79.28; H, 8.49; 5.57; IR (KBr) cm^{-1} 3313, 1651; UV λ_{max} ($CHCl_3$)/nm 417 (ε/dm^3 mol^{-1} cm^{-1} 142184), 515 (16564), 549 (6591), 590 (5863); δ_H (400 MHz, 3.2 mM in $CDCl_3$) 8.94–8.77 (4 H, m), 8.77–8.62 (4 H, m), 8.09–7.96 (2 H, m), 7.93–7.84 (2 H, m), 7.60–7.49 (2 H, m), 7.47–7.37 (2 H, m), 7.10–6.95 (2 H, m), 6.80–6.69 (2 H, m), 4.33–4.12 (8 H, m), 2.06–1.76 (20 H, m), 1.73–1.11 (56 H, m), 1.00–0.74 (12 H, m), −2.72–(−2.80) (2 H, m); HRMS (FAB+) *m*/*z* calc. for $C_{98}H_{124}N_6O_6$ $[M]^+$: 1480.9582; found 1480.9595.

[5,15-Bis(3-decyloxy-5-[2-oxopyrid-4-yl]phenyl)-10,2-bis(4-decyloxy-2,6-dimethylphenyl)porphyrinato]zinc(II) (3). Porphyrin **5** (110.5 mg, 0.075 mmol) and $Zn(OAc)_2{\cdot}2H_2O$ (40.9 mg, 0.186 mmol) were dissolved in chloroform–methanol 9 : 1 (74 mL) and the reaction mixture was refluxed for 1 h. After cooling to rt, the reaction mixture was extracted several times with 10% $NaHCO_3$, dried ($MgSO_4$) and the solvent was evaporated to afford 116 mg (quantitative) of **3** as a purple solid: Anal. calc. for $C_{98}H_{122}N_6O_6Zn$: C, 76.16; H, 7.96; N, 5.44; found C, 75.86; H, 8.08; N, 5.33; UV λ_{max} ($CHCl_3$)/nm 428 (ε/dm^3 mol^{-1} cm^{-1} 134092), 560 (18336), 599 (5492); IR (KBr) cm^{-1} 3413, 1651; δ_H (400 MHz, 4.6 mM in $CDCl_3$–pyridine-d_5; 94.8%) 8.94–8.77 (4 H, m), 8.77–8.62 (4 H, m), 8.09–7.96 (2 H, m), 7.93–7.84 (2 H, m), 7.60–7.49 (2 H, m), 7.47–7.37 (2 H, m), 7.10–6.95 (2 H, m), 6.80–6.69 (2 H, m,), 4.33–4.12 (8 H, m) 2.06–1.70 (20 H, m), 1.73–1.11 (56 H, m), 1.00–0.74 (12 H, m); HRMS (FAB+) *m*/*z* calc. for $C_{98}H_{122}N_6O_6Zn$ $[M]^+$: 1542.8717; found 1542.8716.

1,4-Diphenyl-1-*Z*-butene (6). Freshly distilled morpholine (4.75 mL, 54.0 mmol) was added to a solution of 1,4-diphenylbutane-1-one (**42**, 2.02 g, 9.00 mmol) in anhydrous benzene (20 mL) under argon. $TiCl_4$ (560 μL, 5.08 mmol) was then slowly added, resulting in the formation of a precipitate and a slight temperature increase. The mixture was left stirring overnight at rt. The formed precipitates of TiO_2 and morpholinium chloride were removed by filtration after the addition of hexane (20 mL). The filter cake was washed with hexane (2 × 10 mL). The filtrate was concentrated and the residue was dissolved in the minimum amount of warm hexane (*ca.* 10–20 mL) and any insoluble residues filtered off. Evaporation of the solvent afforded 2.48 g (8.45 mmol, 94%) of pure enamine **43** as a light yellow solid: δ_H (300 MHz, $CDCl_3$) 7.40–7.20 (8 H, m), 7.09 (2 H, d, J = 7.0 Hz), 4.63 (1 H, t, J = 7.4 Hz), 3.69 (4 H, t, J = 4.8 Hz), 2.70 (4 H, t, J = 4.8 Hz), 2.63 (2 H, t, J = 7.7 Hz), 2.25 (2 H, dt, J = 7.7 Hz, J = 7.4 Hz); HRMS (EI+) *m*/*z* calc. for $C_{20}H_{23}NO$ $[M]^+$: 293.1780; found 293.1775. The solid was dried *in vacuo* for 2 h and then dissolved in anhydrous THF (3 mL). This solution was transferred *via* syringe to another flask containing solid 9-BBN (1.03 g, 8.45 mmol). The original flask was washed with THF (1 mL) and the washings were transferred to the reaction flask. The resulting suspension was stirred for 3 h at rt, during which it became a clear yellow solution. After evaporating the solvent at rt, the sticky residue was treated with dry methanol (685 μL, 16.9 mmol). An exothermic reaction was initiated by gentle warming with a heat gun, initially liquefying, but within 2 min, solidifying the contents of the flask. The solid residue was triturated with hexane (3 × 10 mL). The combined hexane solutions were washed with 3 M NaOH (3 × 5 mL) and water (2 × 5 mL), dried ($MgSO_4$) and evaporated to give a light yellow oil. Purification by chromatography (6 × 10 cm, eluent: heptane) afforded 1.16 g (66%) of **6** as a colorless liquid: R_f (heptane–EtOAc 4 : 1) 0.64; anal. calc. for $C_{16}H_{16}$: C, 92.26; H, 7.74; found C, 92.13; H, 7.76; IR (neat film) cm^{-1} 2922, 2855, 1601, 1493, 1452; δ_H (400 MHz, $CDCl_3$) 7.35–7.19 (10 H, m), 6.46 (1 H, d, J = 11.7 Hz), 5.72 (1 H, dt, J = 11.7, J = 7.1 Hz), 2.78 (2 H, m), 2.69 (2 H, m); δ_C (100 MHz, $CDCl_3$) 141.7, 137.5, 131.8, 129.4, 128.7, 128.5, 128.3, 128.1, 126.6, 125.9, 36.1, 30.4; HRMS (FAB+) *m*/*z* calc. for $C_{16}H_{16}$ $[M]^+$: 208.1252; found 208.1251.

4-(4-Phenyl-*Z*-but-3-enyl)pyridine (7). The title compound was prepared according to the same procedure as compound **6**, from 1-phenyl-4-pyridin-4-ylbutan-1-one (**40**, 4.51 g, 20.0 mmol), $TiCl_4$ (1.24 mL, 11.2 mmol), morpholine (10.6 mL, 120 mmol) in benzene (40 mL), *via* the enamine intermediate **44** (4.71 g, 16.0 mmol, 80%): mp 74–75 °C; anal. calc. for $C_{19}H_{22}N_2O$: C, 77.52; H, 7.53; N, 9.52; found C, 77.65; H, 7.42; N, 9.44; δ_H (400 MHz, $CDCl_3$) 8.44 (2 H, d, J = 6.0 Hz), 7.35–7.28 (3 H, m), 7.20 (2 H, d, J = 6.0 Hz), 6.98 (2 H, d, J = 6.0 Hz), 4.55 (1 H, t, J = 7.4 Hz), 3.68 (4 H, t, J = 4.8 Hz), 2.68 (4 H, t, J = 4.8 Hz), 2.60 (2 H, t, J = 7.6 Hz), 2.26 (2 H, dt, J = 7.6 Hz, J = 7.4 Hz); δ_C (100 MHz, $CDCl_3$) 150.9, 150.7, 149.5, 137.3, 129.6, 128.1, 127.7, 124.0, 103.6, 67.0, 49.7, 36.7, 28.9; HRMS (EI+) *m*/*z* calc. for $C_{19}H_{22}N_2O$ $[M]^+$: 294.1732; found 294.1729. Enamine **44**, together with 9-BBN (3.90 g, 32.0 mmol, 2 equiv.) in THF (8 mL), followed by MeOH (1.30 mL, 32.0 mmol) then afforded, after purification by chromatography (6 × 9 cm, eluent: heptane–EtOAc 1 : 4), 1.07 g (32%) of **7** as a colorless liquid: Anal. calc. for $C_{15}H_{15}N$: C, 86.08; H, 7.22; N, 6.69; found C, 85.92; H, 7.16; N 6.73; IR (neat film) cm^{-1} 1601, 1558, 1493, 1446, 1413; δ_H (400 MHz, $CDCl_3$) 8.49 (2 H, d, J = 6.0 Hz), 7.37–7.29 (2 H, m), 7.26–7.19 (3 H, m), 7.11 (2 H, d, J = 6.0 Hz), 6.48 (1 H, d, J = 11.6 Hz), 5.65 (1 H, dt, J = 11.6, J = 7.0 Hz), 2.77 (2 H, m), 2.68 (2 H, m); δ_C (100 MHz, $CDCl_3$) 150.6, 149.6, 137.2, 130.6, 130.2, 128.6, 128.2, 126.8, 123.9, 35.3, 29.0; HRMS (EI+) *m*/*z* calc. for $C_{15}H_{15}N$ $[M]^+$: 209.1204; found 209.1208.

1-Phenyl-5-(pyridin-4-yl)pentan-1-one (41). Freshly cut pieces of sodium (1.26 g, 54.8 mmol) were slowly added to dried abs. EtOH (15 mL), followed by addition of ethyl benzoylacetate (12.9 g, 67.2 mmol), resulting in a clear solution. 4-(3-Bromopropyl)pyridinium chloride (14.0 g, 49.8 mmol) was treated with toluene (60 mL) and 1 M NaOH (60 mL). The phases were separated and the aqueous phase was extracted with toluene (2 × 40 mL). The combined organic phases were dried (Na_2SO_4) and concentrated to a volume of 30–40 mL during which the solution turned dark and a small amount of black precipitate formed. This dark solution was added to the reaction mixture, which took a green color. It was refluxed for 4 h, during which it turned red and highly turbid. After cooling to rt, water (100 mL) was added and the mixture was acidified to pH 2 by adding conc. HCl. The phases were separated and the acidic water phase was washed with ether (2 × 60 mL). It was then basified by addition of solid K_2CO_3 and extracted with ether (3 × 60 mL). The combined basic extracts were dried (Na_2SO_4) and concentrated to yield a dark brown oil which was dissolved in 6 M HCl (50 mL) and refluxed for 6 h. At rt, the mixture was basified with 10 M NaOH and extracted ether (3 × 50 mL). The combined organic phases were dried (Na_2SO_4) and concentrated to yield 6.4 g of a dark oil containing **41**. Chromatography (5 × 15 cm, eluent: EtOAc)

did not result in a pure product due to a coeluting impurity. 4 M HCl in dioxane (9 mL, 36 mmol) was added to a solution of crude **41** in ether (50 mL), resulting in the precipitation of **41**·HCl, which could be purified by recrystallization from MeCN (120 mL), affording 5.1 g of pure **41**·HCl. Basifying with 1 M NaOH (60 mL) and extracting with ether (3 × 40 mL), drying (Na_2SO_4) and concentrating provided 3.75 g (31%) of pure **41** as a colorless oil that slowly crystallized: mp 41–43 °C; anal. calc. for $C_{16}H_{17}NO$: C, 80.30; H, 7.16; N, 5.85; found C, 80.05; H, 7.15; N, 5.96; IR (KBr) cm^{-1} 1684, 1601, 1445, 1416; δ_H (400 MHz, $CDCl_3$) 8.48 (2 H, d, $J = 6.0$ Hz), 7.94 (2 H, d, $J = 8.2$ Hz), 7.56 (1 H, t, $J =$ 7.4 Hz), 7.46 (2 H, dt, $J = 8.2$ Hz, $J = 7.4$ Hz), 7.11 (2 H, d, $J =$ 6.0 Hz), 3.0 (2 H, t, $J = 7.0$ Hz), 2.66 (2 H, t, $J = 7.4$ Hz), 1.85–1.65 (4 H, m); δ_C (100 MHz, $CDCl_3$) 199.8, 151.1, 149.6, 136.9, 133.0, 128.6, 127.9, 123.8, 38.1, 35.1, 29.8, 23.7; HRMS (EI+) *m/z* calc. for $C_{16}H_{17}NO$ $[M]^+$: 239.1310; found 239.1309.

4-(5-Phenyl-*Z*-pent-4-enyl)pyridine (8). The title compound was prepared according to the same procedure as compound **6**, from ketone **41** (2.15 g, 8.98 mmol), $TiCl_4$ (560 μL, 5.08 mmol), morpholine (4.75 mL, 54.0 mmol) in benzene (20 mL), *via* the enamine intermediate **45** (2.51 g, 8.12 mmol, 90%): δ_H (400 MHz, $CDCl_3$) 8.42 (2 H, d, $J = 6.0$ Hz), 7.37–7.25 (5 H, m), 7.00 (2 H, d, $J = 6.0$ Hz), 4.58 (1 H, t, $J = 7.4$ Hz), 3.70 (4 H, t, $J = 4.8$ Hz), 2.69 (4 H, t, $J = 4.8$ Hz), 2.51 (2 H, t, $J = 7.7$ Hz), 1.99 (2 H, dt, $J = 7.4$ Hz, $J = 7.3$ Hz), 1.65 (2 H, tt, $J = 7.7$ Hz, $J = 7.3$ Hz); δ_C (100 MHz, $CDCl_3$) 151.4, 150.2, 149.5, 137.6, 129.6, 128.0, 127.6, 123.8, 104.9, 67.1, 49.8, 34.5, 31.7, 27.6; HRMS (EI+) *m/z* calc. for $C_{20}H_{24}N_2O$ $[M]^+$: 308.1889; found 308.1886. Enamine **45**, together with 9-BBN (1.982 g, 16.24 mmol, 2 equiv.) in THF (4 mL), followed by MeOH (659 μL, 16.2 mmol) then afforded, after purification by chromatography (5 × 15 cm, eluent: heptane–EtOAc 1 : 4), 950 mg (52%) of **8** as a colorless liquid: Anal. calc. for $C_{16}H_{17}N$: C, 86.05; H, 7.67; N, 6.27; found C, 85.88; H, 7.63; N 6.34; IR (neat film) cm^{-1} 2934, 2858, 1601, 1558, 1493, 1446, 1413; δ_H (400 MHz, $CDCl_3$) 8.46 (2 H, d, $J = 6.0$ Hz), 7.35–7.21 (5 H, m), 7.06 (2 H, d, $J = 5.9$ Hz), 6.48 (1 H, d, $J = 11.6$ Hz), 5.67 (1 H, dt, $J = 11.6$, $J = 7.3$ Hz), 2.63 (2 H, t, $J = 7.6$ Hz), 2.38 (2 H, dtt, $J = 7.4$, $J = 7.3$, $J = 1.7$ Hz), 1.80 (2 H, tt, $J = 7.4$, $J =$ 7.3 Hz); δ_C (100 MHz, $CDCl_3$) 151.1, 149.6, 131.8, 129.7, 128.7, 128.2, 126.6, 123.9, 34.6, 30.5, 27.8; HRMS (FAB+) *m/z* calc. for $C_{16}H_{18}N$ $[M + 1]^+$: 224.1439; found 224.1431.

4-(4-*tert*-Butylphenyl)pyridine (46). A two phase mixture of 4-*tert*-butylphenylboronic acid (1.0 g, 5.6 mmol), 4-bromopyridinium chloride (0.99 g, 5.9 mmol), Na_2CO_3 (1.78 g, 16.8 mmol), benzene (11 mL) and water (5 mL) was degassed by bubbling argon through it for 15 min. $Pd(PPh_3)_4$ (194 mg, 0.168 mmol) was then added and the mixture was refluxed under argon overnight. After cooling to rt, water (15 mL) was added and the mixture was extracted with EtOAc (3 × 15 mL). The combined organic phases were dried ($MgSO_4$) and concentrated. The residue was purified by chromatography (4 × 18 cm, eluent: heptane–EtOAc gradient from 7 : 3 to 0 : 1), affording 956 mg (80%) of **46** as a white solid: Anal. calc. for $C_{15}H_{17}N$: C, 85.26; H, 8.11; N, 6.63; found C, 85.30; H, 8.04; N, 6.58; δ_H (400 MHz, $CDCl_3$) 8.65 (2 H, d, $J = 6.1$ Hz), 7.60 (2 H, d, $J = 8.5$ Hz), 7.53 (2 H, d, $J = 8.5$ Hz), 7.52 (2 H, d, $J = 6.1$ Hz), 1.38 (9 H, s); δ_C (100 MHz, $CDCl_3$) 152.4, 150.1, 148.2, 135.12, 126.6, 126.1, 121.4, 34.7, 31.3; HRMS (FAB+) *m/z* calc. for $C_{15}H_{18}N$ $[M + 1]^+$: 212.1439; found 212.1439.

4-(4-*tert*-Butylphenyl)pyridine *N*-oxide (12). MTO (2.7 mg, 0.011 mmol) was added to a solution of pyridine **46** (448 mg, 2.12 mmol), in CH_2Cl_2 (0.85 mL) followed by dropwise addition of 30% H_2O_2 (425 μL, 4.25 mmol). Evolution of heat and gas was observed. The reaction mixture was stirred at rt for 24 h. A grain of MnO_2 was then added to destroy excess H_2O_2, the mixture was stirred for 1 h. Water (10 mL) and CH_2Cl_2 (10 mL) were added and the phases were separated. The aqueous phase was extracted with CH_2Cl_2 (2 × 10 mL). The combined organic phases were dried (Na_2SO_4) and concentrated. The residue was recrystallized from hexane–benzene 3 : 1 (30 mL) affording 357 mg (74%) of **12** as an off-white solid: mp 147–148 °C (hexane–benzene 3 : 1); anal. calc. for $C_{15}H_{17}NO$: C, 79.26; H, 7.54; N, 6.16; found C, 79.20; H, 7.62; N 6.19; IR (KBr) cm^{-1} 1481, 1246; δ_H (400 MHz, $CDCl_3$) 8.24 (2 H, bs), 7.6–7.4 (6 H, bs), 1.37 (9 H, s); δ_C (100 MHz, $CDCl_3$) 152.7, 139.5, 138.8, 133.1, 126.3, 126.1, 123.3, 34.7, 31.2; HRMS (FAB+) *m/z* calc. for $C_{15}H_{18}NO$ $[M + 1]^+$: 228.1383; found 228.1388.

Epoxidations

Substrate- and enantioselectivity at different temperatures

Typically, these reactions were run in pairs, one with and one without receptor **3**. Catalyst **2** (4.59 mg, 3.00 μmol) was weighed into two 2 mL glass vials. Receptor **3** (4.64 mg, 3.00 μmol) was added to one of the vials. A 1 mL stock solution of benzyl benzoate (IS, 44.9 mM), *N*-oxide **12** (35.9 mM) and two substrates (**5**, 90.0 mM and **6**, 90.0 mM) in $CDCl_3$ was prepared. 333 μL of the stock solution were transferred to each vial followed by 267 μL of $CDCl_3$. Homogeneous solution was obtained after ultrasonication. Into another pair of vials, PhIO (2.64 mg, 12.0 μmol) was weighed and the reaction solutions were transferred to the PhIO containing vials after equilibrating to the appropriate temperature (see Table 3).

A typical reaction mixture thus contained the following: Substrate **6** (30 μmol), substrate **7** (30 μmol), catalyst **2** (3 μmol), receptor **3** (3 μmol), PhIO (12 μmol), *N*-oxide **12** (12 μmol), benzyl benzoate (15 μmol) and $CDCl_3$ (0.6 mL). After stirring for 24 h, each reaction mixture was concentrated to dryness, suspended in EtOAc (1 mL) with the aid of ultrasonication, then applied to a dry 1.2 g silica pad (0.5 cm diameter) and eluted with EtOAc (25 mL). After evaporation of the solvent, the residue was dissolved in ether (1 mL) and membrane filtered to remove any residual catalyst. The ether was evaporated and the residue dissolved in $CDCl_3$ (0.8 mL) for NMR analysis. An aliquot was taken for GC analysis to estimate the substrate selectivity and the ee of epoxide **10**. After analysis of the NMR sample, it was evaporated and epoxide **9** was separated from **10** by chromatography (0.5 × 6 cm, eluent: heptane–EtOAc 8 : 2) to be able to measure the ee of **9** by GC.

For the estimation of substrate selectivity the following GC method was used. Carrier gas: helium. Flow gradient: 0.5 to 3 mL min^{-1} ramp 0.1. Oven program: 140 to 185 °C ramp 3, then to 250 °C ramp 10 °C per min, then hold 3.5 min. Total time: 25 min. Retention times of substrates and internal standard (IS) were as follows: IS: 12.7 min, **6**: 12.5 min, **7**: 14.7 min, **8**: 16.7 min. *cis*-Epoxide products had the following retention times: **9**: 14.9 min, **10**: 16.7 min, **11**: 18.2 min. *cis*-Epoxide peaks

consistently accounted for approximately 70% of total area of all detectable product peaks. For the estimation of enantioselectivity the following GC methods were used: Oven program for **9** and **11**: isotherm 150 °C. Retention time of enantiomers: **9** 127.7 and 132.2 min and **11** 194.2 and 195.9 min. Oven program: for **10**: isotherm 170 °C. Retention times of the enantiomers of **10** were 106.6 and 109.3 min.

Reactivity and stability studies

Four stock solutions in CH_2Cl_2 were prepared: benzyl benzoate (0.1 M), *N*-oxide **12** (0.82 M), substrate **7** (0.2 M) and substrate **6** (0.2 M). 0.2 mL of each of the required stock solutions were transferred to the reaction vials (see Table 4) and CH_2Cl_2 was added where needed to complete the reaction volume to 0.8 mL. Homogeneous solution was obtained after ultrasonication. 0.6 mL of the reaction solutions were transferred to vials containing PhIO (14.5 mg, 0.066 mmol).

A typical reaction mixture thus contained the following: olefins (**6** and/or **7**, 60 μmol total), **2** (3 μmol), **3** (3 μmol), PhIO (66 μmol), *N*-oxide **12** (12 μmol), benzyl benzoate (15 μmol) and CH_2Cl_2 (0.6 mL).

Aliquots (20 μL) were taken for analysis after 1, 15, 60 and 240 min. Each aliquot was added to ether (0.25 mL) to precipitate **2** and was filtered through a short pad of silica gel and eluted with ether (3 × 0.25 mL). The so obtained sample was analysed by GC, using the same method as in substrate selectivity studies.

Turnover number experiments

Catalyst **2** (1.53 mg, 1.00 μmol), receptor **3** (6.24 mg, 4.00 μmol), styrene (52.1 mg, 0.500 mmol), naphthalene (IS, 12.8 mg, 0.100 mmol), *N*-oxide **12** (0.9 mg, 4 μmol) and 4-ethylpyridine (10.7 mg, 0.100 mmol) were dissolved in CH_2Cl_2 (1 mL). PhIO (22.0 mg, 0.100 mmol) was added every 30 min. An aliquot (20 μL) was taken after 1, 15, 60, 120, 180 and 300 min and was treated as above to obtain a GC sample. The following GC method was used. Carrier gas: helium. Flow: 1 mL min^{-1}. Oven program: 60 to 160 °C ramp 10. Total time: 10 min. Retention times of styrene, benzaldehyde, styrene oxide and naphtalene (IS) were as follows: styrene: 4.54 min, benzaldehyde: 5.26 min, styrene oxide: 6.72 min and IS: 8.47 min (Table 5).

Acknowledgements

We are grateful to Dr Karl-Erik Bergquist for his expert assistance on quantitative NMR analysis and to Dr Tobias Ryden as well as to Susann Stjernqvist for their generous help with the mathematics and computation of standard errors for the mole fractions and confidence intervals for the association constants. We thank the Swedish Research Council as well as the Crafoord Foundation, the Lars-Johan Hierta Foundation, the Magn. Bergvall Foundation, the Royal Physiographic Society, and the Danish Research Council for Technology and Production Sciences for grants.

References

1 For reviews on the subject, see: (*a*) M. J. Wilkinson, P. W. N. M. v. Leeuwen and J. N. H. Reek, *Org. Biomol. Chem.*, 2005, **3**, 2371; (*b*) W. B. Motherwell, M. J. Bingham and Y. Six, *Tetrahedron*, 2001, **57**, 4663; (*c*) J. K. M. Sanders, *Chem.–Eur. J.*, 1998, **4**, 1378; (*d*) M. C. Feiters, in *Comprehensive Supramolecular Chemistry*, ed. D. N. Reinhoudt, Elsevier, Oxford, 1996, pp. 267–360; (*e*) A. J. Kirby, *Angew. Chem., Int. Ed. Engl.*, 1996, **35**, 707; (*f*) Y. Murakami, J.-i. Kikuchi, Y. Hisaeda and O. Hayashida, *Chem. Rev.*, 1996, **96**, 721; (*g*) R. Breslow, *Acc. Chem. Res.*, 1995, **28**, 146.
2 J.-M. Lehn, *Supramolecular Chemistry: Concepts and Perspectives*, VCH, Weinheim, 1995.
3 D. Fiedler, R. G. Bergman and K. N. Raymond, *Angew. Chem., Int. Ed.*, 2004, **43**, 6748; J. Yang and R. Breslow, *Angew. Chem., Int. Ed.*, 2000, **39**, 2692; P. Mattei and F. Diederich, *Helv. Chim. Acta*, 1997, **80**, 1555.
4 S. Jónsson, F. G. J. Odille, P.-O. Norrby and K. Wärnmark, *Chem. Commun.*, 2005, 549.
5 W. Zhang, J. L. Loebach, S. R. Wilson and E. N. Jacobsen, *J. Am. Chem. Soc.*, 1990, **112**, 2801; R. Irie, K. Noda, Y. Ito, N. Matsumoto and T. Katsuki, *Tetrahedron Lett.*, 1990, **31**, 7345.
6 Kinetics of pyridine–Zn(porphyrin) interaction: E. F. Caldin and J. P. Field, *J. Chem. Soc., Faraday Trans. 1*, 1982, **78**, 1923. Kinetics of 2-pyridone self-association:; G. G. Hammes and A. C. Park, *J. Am. Chem. Soc.*, 1969, **91**, 956.
7 A. Ikeda, M. Ayabe, S. Shinkai, S. Sakamoto and K. Yamaguchi, *Org. Lett.*, 2000, **2**, 3707; M. Marty, Z. Clyde-Watson, L. J. Twyman, M. Nakash and J. K. M. Sanders, *Chem. Commun.*, 1998, 2265.
8 Y. Ducharme and J. D. Wuest, *J. Org. Chem.*, 1988, **53**, 5787.
9 F. Mohamadi, N. G. J. Richards, W. C. Guida, R. Liskamp, M. Lipton, C. Caufield, G. Chang, T. Hendrickson and W. C. Still, *J. Comput. Chem.*, 1990, **11**, 440.
10 The modelling was done using a preliminary force-field for transition states in Mn(salen) catalysed epoxidation: P.-O. Norrby, unpublished work.
11 Examples of catalytic systems assembled by hydrogen-bonding: J. Chen and J. Rebek, Jr., *Org. Lett.*, 2002, **4**, 327; K. Ohsaki, K. Konishi and T. Aida, *Chem. Commun.*, 2002, 1690; J. Kang, J. Santamaria, G. Hilmersson and J. Rebek, Jr., *J. Am. Chem. Soc.*, 1998, **120**, 7389.
12 Examples of supramolecular encapsulation of transition metal catalysts: D. H. Leung, D. Fiedler, R. G. Bergman and K. N. Raymond, *Angew. Chem., Int. Ed.*, 2004, **43**, 963; N. C. Gianneschi, P. A. Bertin, S. T. Nguyen, C. A. Mirkin, L. N. Zakharov and A. L. Rheingold, *J. Am. Chem. Soc.*, 2003, **125**, 10508; V. F. Slagt, P. W. N. M. van Leeuwen and J. N. H. Reek, *Angew. Chem., Int. Ed.*, 2003, **42**, 5619; M. L. Merlau, M. Del Pilar Mejia, S. T. Nguyen and J. T. Hupp, *Angew. Chem., Int. Ed.*, 2001, **40**, 4239.
13 S. C. Zimmerman and B. F. Duerr, *J. Org. Chem.*, 1992, **57**, 2215.
14 K. M. Tramposch, H. F. Kung and M. Blau, *J. Med. Chem.*, 1983, **26**, 121.
15 E. J. Corey, D.-H. Lee and S. Sarshar, *Tetrahedron: Asymmetry*, 1995, **6**, 3; S. Pikul and E. J. Corey, *Org. Synth.*, 1993, **71**, 22.
16 B. Wappes, M. Jennerwein, E. Von Angerer, H. Schoenenberger, J. Engel, M. Berger and K. H. Wrobel, *J. Med. Chem.*, 1984, **27**, 1280.
17 P. Rocca, C. Cochennec, F. Marsais, L. Thomas-dit-Dumont, M. Mallet, A. Godard and G. Queguiner, *J. Org. Chem.*, 1993, **58**, 7832.
18 I. Paterson, C. J. Cowden, V. S. Rahn and M. D. Woodrow, *SYNLETT*, 1998, 915.
19 S. Hünig and H. Schwarz, *Justus Liebigs Ann. Chem.*, 1956, **599**, 131.
20 B. J. Littler, M. A. Miller, C.-H. Hung, R. W. Wagner, D. F. O'Shea, P. D. Boyle and J. S. Lindsey, *J. Org. Chem.*, 1999, **64**, 1391.
21 B. J. Littler, Y. Ciringh and J. S. Lindsey, *J. Org. Chem.*, 1999, **64**, 2864.
22 B. Singaram, M. V. Rangaishenvi, H. C. Brown, C. T. Goralski and D. L. Hasha, *J. Org. Chem.*, 1991, **56**, 1543; B. Singaram, C. T. Goralski, M. V. Rangaishenvi and H. C. Brown, *J. Am. Chem. Soc.*, 1989, **111**, 384.
23 R. Stradi, D. Pocar and C. Cassio, *J. Chem. Soc., Perkin Trans. 1*, 1974, 2671.
24 C. Coperet, H. Adolfsson, T.-A. V. Khuong, A. K. Yudin and K. B. Sharpless, *J. Org. Chem.*, 1998, **63**, 1740.
25 R. B. Martin, *Chem. Rev.*, 1996, **96**, 3043.
26 F. G. J. Odille, *Investigation of Kinetically Labile Supramolecular System Addressing Substrate Selectivity in the Catalytic Epoxidations of Olefins*, PhD thesis, Lund University, 2006, ISBN 91-7422-104-3.
27 M. Palucki, N. S. Finney, P. J. Pospisil, M. L. Gueler, T. Ishida and E. N. Jacobsen, *J. Am. Chem. Soc.*, 1998, **120**, 948.
28 (*a*) T. Katsuki, in *Catalytic Asymmetric Synthesis,, 2nd edn*, ed. I. Ojima, Wiley-VCH, New York, 2000, ch. 6B; (*b*) E. N. Jacobsen and M. H. Wu,

in *Comprehensive Asymmetric Catalysis*, ed. E. N. Jacobsen, A. Pfaltz and H. Yamamoto, Springer-Verlag, 1999, ch. 18.2.
29 (*a*) C. Linde, M. Arnold, P. O. Norrby and B. Åkermark, *Angew. Chem., Int. Ed. Engl.*, 1997, **36**, 1723; (*b*) C. Linde, B. Åkermark, P.-O. Norrby and M. Svensson, *J. Am. Chem. Soc.*, 1999, **121**, 5083–5084; (*c*) C. Linde, N. Koliai, P. O. Norrby and B. Åkermark, *Chem.–Eur. J.*, 2002, **8**, 2568–2573; (*d*) P. Fristrup, B. B. Dideriksen, D. Tanner and P.-O. Norrby, *J. Am. Chem. Soc.*, 2005, **127**, 13672–13679.
30 E. M. McGarrigle and D. G. Gilheany, *Chem. Rev.*, 2005, **105**, 1563.
31 K. Srinivasan, P. Michaud and J. K. Kochi, *J. Am. Chem. Soc.*, 1986, **108**, 2309.
32 W. Adam, K. J. Roschmann, C. R. Saha-Moeller and D. Seebach, *J. Am. Chem. Soc.*, 2002, **124**, 5068.
33 J. P. Collman, L. Zeng and J. I. Brauman, *Inorg. Chem.*, 2004, **43**, 2672.
34 J. R. Chipperfield, J. Clayton, S. A. Khan and S. Woodward, *J. Chem. Soc., Dalton Trans.*, 2000, 1087.
35 Unambiguous proof that *N*-oxide ligands coordinate to O=Mn(v)(salen) species during the oxygen transfer step was provided both by Jacobsen: N. S. Finney, P. J. Pospisil, S. Chang, M. Palucki, R. G. Konsler, K. B. Hansen and E. N. Jacobsen, *Angew. Chem., Int. Ed. Engl.*, 1997, **36**, 1720; and by Katsuki:; K. Miura and T. Katsuki, *SYNLETT*, 1999, 783.
36 D. Feichtinger and D. A. Plattner, *Chem.–Eur. J.*, 2001, **7**, 591.
37 L. Cavallo and H. Jacobsen, *Inorg. Chem.*, 2004, **43**, 2175.
38 For example: G. A. Morris, S. T. Nguyen and J. T. Hupp, *J. Mol. Catal. A: Chem.*, 2001, **174**, 15.
39 J. El-Bahraoui, O. Wiest, D. Feichtinger and D. A. Plattner, *Angew. Chem., Int. Ed.*, 2001, **40**, 2073.
40 T. Hamada, T. Fukuda, H. lmanishi and T. Katsuki, *Tetrahedron*, 1996, **52**, 515–530.
41 (*a*) H. Buschmann, H.-D. Scharf, N. Hoffmann, M.-W. Plath and J. Runsink, *J. Am. Chem. Soc.*, 1989, **111**, 5367; (*b*) H. Buschmann, H.-D. Scharf, N. Hoffmann and P. Esser, *Angew. Chem., Int. Ed. Engl.*, 1991, **103**, 480; (*c*) K. J. Hale and J. R. Ridd, *J. Chem. Soc., Chem. Commun.*, 1995, 357; (*d*) K. J. Hale and J. R. Ridd, *J. Chem. Soc., Perkin Trans. 2*, 1995, 1601; (*e*) A. Gypser and P.-O. Norrby, *J. Chem. Soc., Perkin Trans. 2*, 1997, 939–943.
42 N. S. Finney, P. J. Pospisil, S. Chang, M. Palucki, R. G. Konsler, K. B. Hansen and E. N. Jacobsen, *Angew. Chem., Int. Ed. Engl.*, 1997, **36**, 1720–1723.
43 M. Cavazzini, A. Manfredi, F. Montanari, S. Quici and G. Pozzi, *Eur. J. Org. Chem.*, 2001, 4639.
44 K. Subba Reddy, L. Sola, A. Moyano, M. A. Pericas and A. Riera, *Synthesis*, 2000, 165.
45 P. Brandt, P. O. Norrby, Adrian M. Daly and Declan G. Gilheany, *Chem.–Eur. J.*, 2002, **8**, 4299–4307.
46 H. Saltzman and J. G. Sharefkin, in *Organic Syntheses Collective Vol. V*, ed. H. E. Baumgarten, John Wiley & Sons, New York, 1973, pp. 658–659.

